

**Organic Field-Effect Transistors-Based Gas Sensors**

Journal:	<i>Chemical Society Reviews</i>
Manuscript ID:	CS-TRV-09-2014-000326.R1
Article Type:	Tutorial Review
Date Submitted by the Author:	08-Feb-2015
Complete List of Authors:	Zhang, Congcong; Tianjin University, Department of Chemistry, School of Science & Collaborative Innovation Center of Chemical Science and Engineering (Tianjin) Chen, Penglei; Chinese Academy of Sciences, Institute of Chemistry, and Department of Chemistry, School of Science & Collaborative Innovation Center of Chemical Science and Engineering (Tianjin), Tianjin University, Tianjin 300072, People's Republic of China., Hu, Wenping; Tianjin University,

Cite this: DOI: 10.1039/c0xx00000x

www.rsc.org/xxxxxx

TUTORIAL REVIEW

Organic Field-Effect Transistors-Based Gas Sensors

Congcong Zhang,^a Penglei Chen^{*ab} and Wenping Hu^{ab}

Received (in XXX, XXX) Xth XXXXXXXXX 20XX, Accepted Xth XXXXXXXXX 20XX

DOI: 10.1039/b000000x

5 Organic field-effect transistors (OFETs) are one of the key components of modern organic electronics. While the past several decades have witnessed huge successes in high-performance OFETs, their sophisticated functionalization with regard to the responses towards external stimulations, has also aroused increasing attention and become an important field of general concern. This is promoted by the inherent merits of organic semiconductors, including considerable variety in molecular design, low cost,
10 lightweight, mechanical flexibility, solution processability, *etc.*, and also to the intrinsic advantage of OFETs, including multiparameter accessibility, ease of large scale manufacturing *etc.*, which provide OFETs with great opportunities as portable yet reliable sensors of high sensitivity, selectivity, and expeditious responses *etc.* With special emphases on the works achieved since 2009, this tutorial review focuses on OFETs-based gas sensors. The working principles of this kind of gas sensors are discussed in
15 detail, the state-of-the-art protocols developed for high-performance gas sensing are highlighted, and the advanced gas discrimination systems in terms of sensory arrays of OFETs are also introduced. This tutorial review intends to provide readers with deep understandings for the future design of high-quality OFET gas sensors of potential uses.

Key learning points

- 20 (1) A general introduction to OFETs and OFET gas sensors.
- (2) Working principles of OFET gas sensors.
- (3) State-of-the-art protocols for high-quality OFET gas sensors.
- (4) Advanced gas discrimination systems in terms of OFET arrays.
- (5) Summary and perspectives of OFET gas sensors.

1. Introduction

Organic field-effect transistors (OFETs), three-terminal electronics using organic semiconductors (OSCs) as active layer, have attracted great expectations from numerous scientific communities.¹⁻⁴ On one hand, OFETs are recognized to be one of
30 the key components of modern electronics. Compared to the inorganic counterparts, their considerable variety in molecular design, low cost, lightweight, mechanical flexibility, low operating voltages, ease of low temperature yet large scale manufacturing *via* inkjet printing and solution processing, and especially their nice compatibility with large-area and flexible substrates/materials, endow them with broad application opportunities in numerous fields of paramount importance. This includes active matrix flat-panel displays, radio frequency
35 identification transponders, light-emitting field-effect transistors, smart cards, *etc.*¹⁻⁴ On the other hand, besides application possibilities, OFETs are also considered to be one of the ideal scientific test-beds for examination, evaluation, identification and optimization of high-quality OSCs.¹ Numerous basic issues of OSCs such as the photophysical processes, charge-transport
40 principles, charge-trapping behaviors *etc.*, have been explored

using OFETs as forum. Thanks to the great achievements in the area of synthesis chemistry, and also to the tremendous progresses made in new fabrication protocols, numerous *ad-hoc*-designed versatile OSCs have been identified *via* OFET
50 investigations.¹⁻³

Over the past several decades, tremendous efforts in terms of design and synthesis of novel OSCs, initiation of new device fabrication protocols, implantation of suitable gate insulator layers, interface engineering, and crystal engineering *etc.*, have
55 witnessed great developments in high-performance OFETs.^{1, 4, 5} Thanks to these advancements, OFETs are currently becoming comparable to or even in sometimes beginning to surpass amorphous silicon thin-film transistors not only in their performances but also with respect to their cost. Practically,
60 one of the most detrimental issues always encountered in OFETs is that their performances are susceptible to chemical interactions, photoexcitation, dimensional deformation, *etc.*, disfavoring their uses in organic circuits.⁶ From another point of view, these undesired issues could be facily utilized to detect external
65 chemical and physical stimuli. The inherent capability of OFETs to directly transform chemical or physical events to the facily read electrical signals renders them potentially applicable for diagnostic uses.⁶ Recently, functionalization of OFETs with

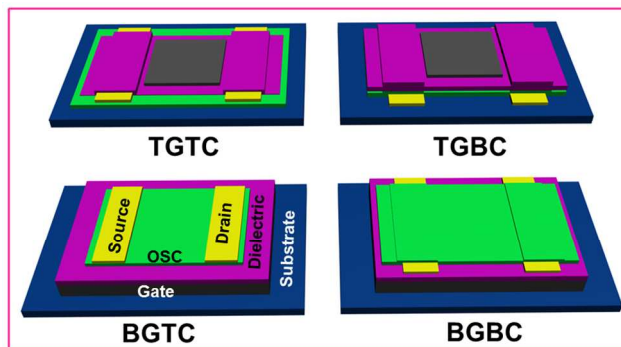
regard to their responses to light, pressure, chemicals, biochemicals *etc.*, have attracted increasing attention and become a focused issue in the interdisciplinary fields of OSCs, organic electronics, materials science, bioscience, sensor science and technology, *etc.*⁶⁻¹⁰

Indeed, compared to OFET sensors, those using inorganic metal oxides as active materials are more stable. However, these inorganic transistors could only exhibit limited selectivity, and a high temperature is generally required for their operations. On one hand, this disfavours their wide applications, especially for the detection of explosive analytes. On the other hand, their high power requirements and consumptions render them not so amenable to minimization, limiting portable and real-time sensing. In contrast, taking into account the intrinsic merits of OSCs, there are many reasons for using OFETs as diagnostic devices. For examples, the huge successes in molecular engineering may confer OSCs with broad diversity in molecular design. This allows the use of *ad-hoc*-designed OSCs, which are functionalized with specific recognition sites or receptors, as the sensory layers, endowing OFET sensors with desirable recognition capability to target analytes. Besides, the good biocompatibility of OSCs over their inorganic counterparts renders OFETs promising candidates not only for physical and chemical sensors but also for biosensors. Moreover, OFET sensors are generally workable at room temperature. This leads to their low energy requirements, facilitating real-time portable sensing. Additionally, OFETs can capitalize on some other advantages of organic materials, such as their mechanical softness, solution processability, low cost, lightweight *etc.*, to hand over flexible and disposable sensors, which are strongly desired for practical uses.

Thus far, lots of room-temperature-operated, low-power-consumption OFET sensors of high sensitivity, expeditious responses, and excellent selectivity have been developed.⁶⁻¹⁰ On account of these progresses, it is appreciated that various OFET sensors are promising component to underpin various future advanced electronics, including phototransistors, electronic skin, tongue, nose *etc.*⁶⁻¹⁰ From the point of view of the form of the diagnostic issues, the numerous relevant literatures could be generally catalogued into several groups: gas sensors, pressure sensors, light sensors, and sensors detecting chemicals or biochemical dispersed in a liquid medium. Several recent reviews summarizing the OFET sensors with particular attention to the detection of light, pressure, and chemicals/biochemicals dissolved in a solution are now available.⁶⁻¹⁰ Although OFET gas sensors have been touched upon frequently as a subsection of some comprehensive reviews,^{2, 6, 8, 10} those themed at this important topic are relatively limited. Considering the significance of functionalization of OFETs, the general interest of gas sensors, and together with the substantial progresses recently achieved in this field, a thematic review on OFET gas sensors is absolutely desired.

With a special emphasis on the state-of-the-art works achieved since 2009, the main aim of this tutorial review is to provide a general overview about the recent progresses in OFET gas sensors. Some historically significant seminal works achieved before 2008, which are of paramount important in shaping this field are also highlighted to provide a foundation. For other

interesting yet earlier studies, we encourage the interested readers to consult other excellent literatures.^{6, 11} This tutorial review is organized as follows. First, the concept of OFETs is presented briefly, followed by a description of how they could work as gas sensors in terms of addressing some sensing mechanisms in details. The advantages and significance of the OFET gas sensors are also spotlighted. Then, we will put emphasis on the impactful protocols of how to improve the performances of the sensors. Subsequently, advanced gas discrimination systems in terms of sensory arrays of OFETs are discussed. In the last section, we put forward an outlook for future directions in this field. We hope that the discussions will be beneficial to future investigations aiming at high-quality OFET gas sensors.



Scheme 1 A schematic illustration of the four typical geometries of OFETs.

2. OFETs: excellent transducer for gas sensing

2.1. A brief introduction to OFETs

Prior to the discussions on OFET gas sensors, a concise introduction to OFETs is necessary. As illustrated in Scheme 1, despite of various possible configurations, such as top-gate top-contact (TGTC), top-gate bottom-contact (TGBC), bottom-gate bottom-contact (BGBC), and bottom-gate top-contact (BGTC) structures, an typical OFET is, in principle, three-terminal electronics, where π -conjugated organic molecules or polymers work as active channel materials, organic or inorganic insulators serve as dielectric layers, and conductive polymers, metals or carbon materials act as source, drain, and gate electrodes. No matter which architecture it is, the active OSC layer, which is located in the channel between source and drain electrodes, is generally isolated from gate electrode by dielectrics. Commonly, the performances of OFETs could be evaluated *via* output and transfer characteristics. The former indicates a plot of source-drain current (I_{DS}) versus source-drain voltage (V_{DS}) at different but constant source-gate voltages (V_{GS}), while the latter represents a plot of I_{DS} versus V_{GS} at constant V_{DS} . The application of a gate bias could induce the formation of a charge accumulation layer at insulator/OSC interface. No current comes into being in the channel when V_{DS} is zero, since the charges along the channel are distributed uniformly in this case. A gradient distribution of the charges along the channel forms when a low V_{DS} , which is smaller than $V_{GS} - V_{Th}$ (V_{Th} stands for threshold voltage), is applied. The result is that the OFET works in linear regime, where its performance follows equation (1). Here, L is channel length, W is channel width, μ represents field-effect

mobility, C_i stands for capacitance per unit area of gate dielectric layer, respectively. During the operation, the current is injected from source electrode into OSC layer, and collected by drain electrode. When a high V_{DS} , which is larger than $V_{GS} - V_{Th}$, is imposed, the device works in saturation region and the I_{DS} herein is given by equation (2). Thus, the conductance of OSC layer could be readily modulated by gate bias with off and on stages

$$I_{DS} = \frac{W}{L} \times \mu C_i (V_{GS} - V_{Th}) \times V_{DS} \quad (1)$$

$$I_{DS} = \frac{W}{2L} \times \mu C_i (V_{GS} - V_{Th})^2 \quad (2)$$

To evaluate the quality of an OFET, the frequently addressed parameters are μ , I_{on}/I_{off} , and V_{Th} etc. The μ could be experimentally derived either *via* transfer characteristics measured with a low V_{DS} in linear regime or those with a high

V_{DS} in saturation region. This parameter, with a unit of $\text{cm}^2 \text{V}^{-1} \text{s}^{-1}$, reflects the absolute value of the velocity to the electric field, and determines the bit speed of the integrated organic circuits, where a μ value as high as possible is wanted. The V_{Th} , which is defined as the minimum V_{GS} required to turn on the transistor, lies mainly on the trap density near the OSC/insulator interface and the quality of source drain contacts. It could be estimated by extrapolating a saturation region transfer curve, which is expressed in the form of a plot of $|I_{DS}|^{1/2}$ versus V_{GS} , to $I_{DS} = 0$. Commonly, a small V_{Th} value is desired, since it means that an OFET could be turned on at a low V_{GS} . The I_{on}/I_{off} refers to the ratio between the highest and the lowest I_{DS} in the range of gate voltage sweep at a certain V_{DS} . It is a crucial factor responsible for switching behaviors of OFETs and their applications in organic digital circuits, OFET-driven organic light emitting diodes etc., where a large I_{on}/I_{off} is desired.

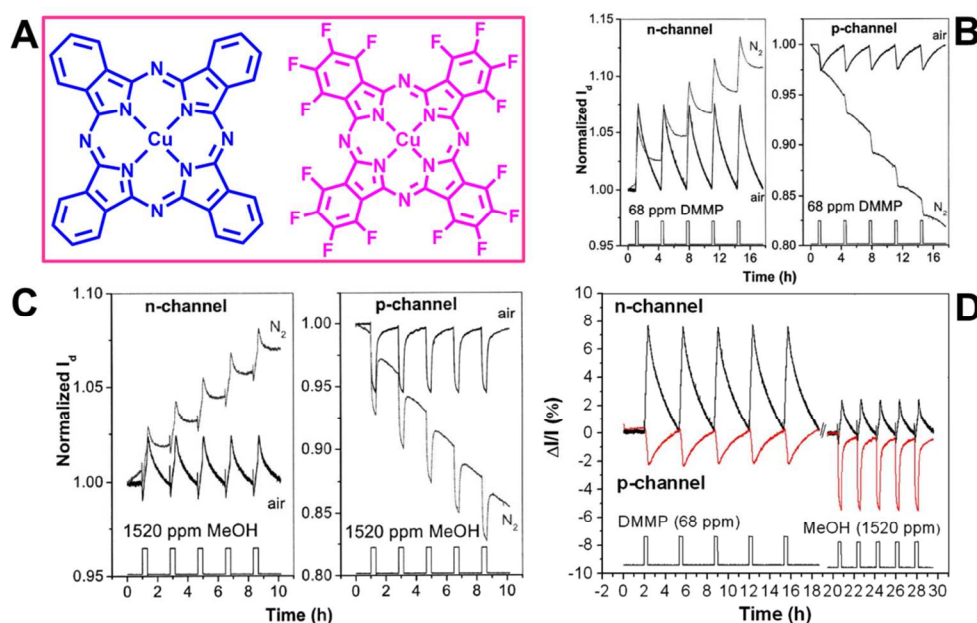


Fig. 1 A typical example showing that the responses of OFET gas sensors strongly depend on the natures of the involved analytes-OSCs pairs. A): Molecular structure of CuPc (*p*-type OSC) and F₁₆CuPc (*n*-type OSC). B and C): The responses of *n*-channel F₁₆CuPc (left) and *p*-channel CuPc (right) OFETs towards DMMP (B) and MeOH (C) in air and N₂. D): The percentage current change of *n*-channel F₁₆CuPc (black) and *p*-channel CuPc (red) OFETs in response to DMMP and MeOH dosing. Copyright 2009, AIP Publishing LLC.

2.2. How could OFETs work as gas sensors?

Since the surroundings we live in are full of gases, and numerous biological and industrial processes are inseparable from gas phase actions, gas sensors are greatly demanded in chemical and pharmaceutical processing, disease diagnostics, national security/defense, food spoilage detection, environmental regulation, pipeline monitoring, etc. Besides OFET gas sensors, which will be the focus of this tutorial review, gas detection could also be achieved by some other protocols or by a combination of these methods, including spectrometry and spectroscopy techniques, gas chromatographic technique, mass-spectrometric technique, surface plasmon resonance technique, optical chemical sensing, mass sensing, etc. These methods are highly selective and sensitive. However, either bulky and expensive equipments or high lever expertise yet tedious operations of these instruments

are required for their operations. This limits their broad uses, especially when real-time and expeditious diagnostics are required. The tremendous progresses in organic electronics provide OFETs with great benefits toward low-cost, portable, and real-time gas sensors. Analyte binding events could be immediately converted to the easily recorded/analyzed electrical signal using OFETs as transducer. Determined by the relative polarity and energy level of the involved analytes and OSCs, and also by the type of the involved OSCs, or by the configuration/structure of the devices etc., these events would lead to changes in electrical performances, rendering OFETs capable of sensing.

So far, numerous works on the transduction mechanism of OFET gas sensors, which is in principle associated with the analytes-devices interactions, has been studied. On one hand, depending on the geometry of the devices and the quality/morphology of the OSCs, these interactions, including

hydrogen bonding, charge transfer, hydrophobic, dipole-dipole interactions *etc.*,¹² could occur on the surface, at the grain boundaries or at various interfaces of OFETs. On the other hand, upon exposure to analytes, the electrical characteristics of OFETs could be affected in terms of trapping, doping, altering the molecular arrangement of the OSC layers, or influencing the charge injection/extraction occurring at electrode/OSC interfaces. Although multiple sensing mechanisms are always responsible for the operation of OFET gas sensors and detailed mechanisms are very complex and are still topics of on-going explorations,¹⁰ they could be, on the whole, divided into two categories, *viz.*, direct and indirect responses.

2.2.1. Direct responses

It is generally accepted that the responses of OFET gas sensors strongly depend on the natures of the involved analytes and OSCs, where different analyte-OSC pairs might display different responses.^{2, 13, 14} A relevant example materializing this issue was reported by Yang *et al.*,¹⁵ where the sensing behaviors of OFETs using copper phthalocyanine (CuPc) and perfluorinated CuPc (F₁₆CuPc), which were *p*- and *n*-type OSCs, respectively, as channel materials (Fig. 1A), were investigated. Using air or N₂ as purge and carrier gases, the CuPc and F₁₆CuPc OFETs exhibited opposite (decreased and increased, respectively) *I*_{DS} changes upon exposure to the tight binding analyte dimethyl methylphosphonate (DMMP, which simulated the phosphonate nerve agents) or to the weak binding analyte MeOH (Fig. 1B-1D), where the analytes worked as hole acceptors and electron donors in *p*- and *n*-type OFETs, respectively. In contrast, the preadsorbed O₂ acted as hole donor and electron trap reagents for *p*- and *n*-channel devices, respectively. The authors described the behaviors of the analytes as “counterdopants” to the preadsorbed O₂, where the analytes may change the delocalized carrier density and/or perturb trap energy of the carriers, leading to *I*_{DS} responses. Moreover, compared to the *p*-channel devices the *n*-channel counterparts displayed larger response to the tight binding analyte DMMP (Fig. 1D). This was attributed to the differences in DMMP perturbation of the electron trap energies versus hole trap energies in the *n*-channel and *p*-channel devices.

Interestingly, compared to the *n*-channel devices, the *p*-channel counterparts exhibited larger response to the weak binding analyte MeOH (Fig. 1D), which was an inverse trend toward the case of the tight binding analyte DMMP. Here, the simulation result indicated a double-exponential process, where fast and slow processes coexisted during the adsorption and desorption. The slow component acted as an electron donor (or hole acceptor) on both the *n*- and *p*-channel devices, resulting a decreased and an increased *I*_{DS} on *p*- and *n*-channel devices, respectively. Conversely, the fast component worked as an electron and hole acceptor on *n*-channel and *p*-channel devices, respectively, unidirectionally decreasing the *I*_{DS} of both the devices. This could be ascribed to the polarity of MeOH molecules, which stabilized holes and electrons in *p*- and *n*-channel devices, respectively, upon weakly physisorbed to the phthalocyanine aromatic rings. The trapping of the free charge carries in the respective devices caused a decrease in current.

The delocalized π -electrons render OSCs susceptible to strong oxidants. This could be utilized to construct OFET sensors with

selectivity towards oxidizing species, where the analytes play a role of electron acceptor (oxidant) in terms of doping the semiconductor or trapping the charges *via* bond cleavage, dipole or complex formation *etc.*¹⁶ The oxidization of OSC could lead to a hole accumulation, conductivity increase, and/or a positively drifted *V*_{Th}, giving out multiparameter sensing readouts. Besides sensors of nice selectivity, this issue in turn provides researchers with good opportunities to disclose the operation mechanisms.

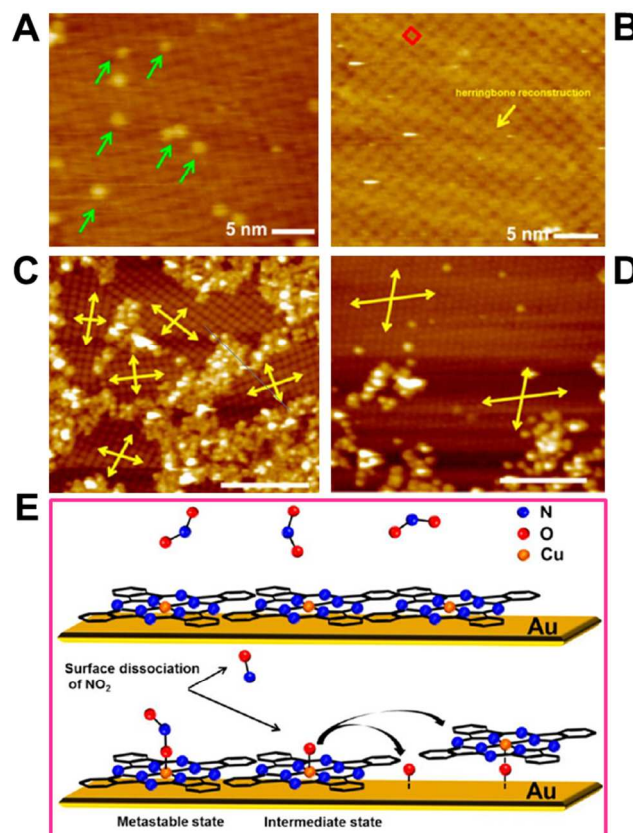


Fig. 2 Dual response mechanism of CuPc OFETs for the dosimetric sensing of NO₂ elucidated by UHV-STM atomic imaging. A and B): STM images of a CuPc monolayer measured after dosing 1 ppm NO₂ at 25 °C and then annealed at 50 °C for 20 min (A) and at 100 °C for 30 min (B). Green arrows indicate chemisorbates. C and D): STM image of a CuPc monolayer measured after dosing 10 ppm NO₂ and then annealed at 50 °C for 10 min (C), and that of the film annealed at 50 °C for 70 min followed by an annealing at 150 °C for 6 h (D). Yellow arrows indicate the orientation of CuPc domains. E): A schematic diagram for domain fracture induced by NO₂ dosing, which renders CuPc OFETs capable of dosimetric sensing NO₂. Copyright 2013, American Chemical Society.

For example,¹⁶ it was reported that vaporous H₂O₂ and organic peroxide (di-tert-butyl peroxide, DTBP) could be selectively detected using *p*-type metal-phthalocyanine (MPc) and naphthalocyanine (Nc) OFETs. When nonoxidizing species such as DMMP and water were sensed, the devices exhibited negative yet reversible responses in $\Delta I_{DS}/I_{DS0}$ and $\Delta\mu/\mu_0$, while *V*_{Th} displayed only a small reversible increase (which might be an artifact of the *I*_{DS}-*V*_{DS} fitting). This was attributed to the characteristic chemisorption events of electron-donating analytes towards *p*-type MPcs *via* preferential binding, leading to the trapping of the carries and thus decreasing the electrical performances. When peroxides were sensed, mobility responses

saturated quickly and were recoverable, indicating the involvement of chemisorption events. In contrast to this reversible issue in mobility, the devices displayed dosimetric responses in V_{Th} and $\Delta I_{DS}/I_{DS0}$ towards peroxide species, both of which exhibited positive, irreversible yet linear drifts with the dose time. A dual response mechanism, where peroxides were chemisorbed and subsequently catalytically decomposed in terms of MPc oxidation and irreversible O–O bond cleavage was proposed. This chemisorptions-oxidation mechanism resulted in the formation of M–O–R species, forming a fixed dipole and causing positive and dosimetric responses in V_{Th} and $\Delta I_{DS}/I_{DS0}$.

Using ultrahigh vacuum scanning tunneling microscopy (UHV–STM), this dual sensing mechanism has recently been further elucidated *via* atomic imaging.¹⁷ For low NO₂ doses (Fig. 2A), isolated chemisorption sites on the center of CuPc were directly verified by STM. An annealing at 100 °C resulted in nearly a complete desorption (Fig. 2B). This corresponded to the observed low-dose reversible changes in mobility. In contrast, high NO₂ doses induced a reorientation of CuPc molecules and a fracture of the CuPc domains, which could only be reversed by an annealing above 150 °C (Fig. 2C, D). This corresponded to the observed high-dose irreversible and dosimetric shifts in V_{Th} . It was proposed that the NO₂ molecules were first reversibly and molecularly chemisorbed to the CuPc metal center, where they dissociated into O and NO accompanied by the generation of O–CuPc complexes (Fig. 2E). This induced the formation of domain fractures together with the irreversible changes in the fixed charge, where the increased density of domain boundaries would act to trap carriers, rendering CuPc OFETs capable of dosimetric sensing NO₂.

Besides the above situations, it has been demonstrated that the mechanism depends also on the dimension (channel length) of the OFETs and the grain size/morphology of the OSCs.^{12, 13, 18, 19} For example, Wang *et al.*¹⁹ investigated the sensing responses of pentacene transistors of various channel lengths and of various pentacene grain size towards 1-pentanol. For nanoscale devices, guard electrodes were implanted at two sides of the channel and kept at the same potential as the drain (Fig. 3A). These two additional electrodes worked as guard conductors to collect the spreading currents originally travelling outside the defined nanochannel such that the direct current from source to drain could be appropriately registered. The use of this four-terminal geometry ensured that the sensor active area was really at nanoscale. Upon exposure to 1-pentanol, decreased and increased I_{DS} were observed from the long and short channel length devices, respectively (Fig. 3B). When pentacene grain size was *ca.* 80 nm (Fig. 3B, top panel), the crossover of these interesting response behaviors occurred in a channel length of *ca.* 150–450 nm. For devices based on larger grain size (*ca.* 250 nm), nearly similar observations were obtained (Fig. 3B, bottom panel), except that the crossover behaviors occurred at larger channel lengths (from 450 nm to 1 μ m). All of the devices with a channel length of $\geq 2 \mu$ m displayed decreased currents upon exposure to analytes no matter the pentacene grain size was at nanoscale (140 nm) or even at micron scale (1 μ m). An interesting phenomenon was that the amplitude of the decreasing signal observed from the 2 μ m channel devices was smaller than those of the longer channel devices, especially for those based on larger pentacene grains (1

μ m). Analogous sensing behaviors were observed from the responses of thiophene OFET gas sensors.¹⁸

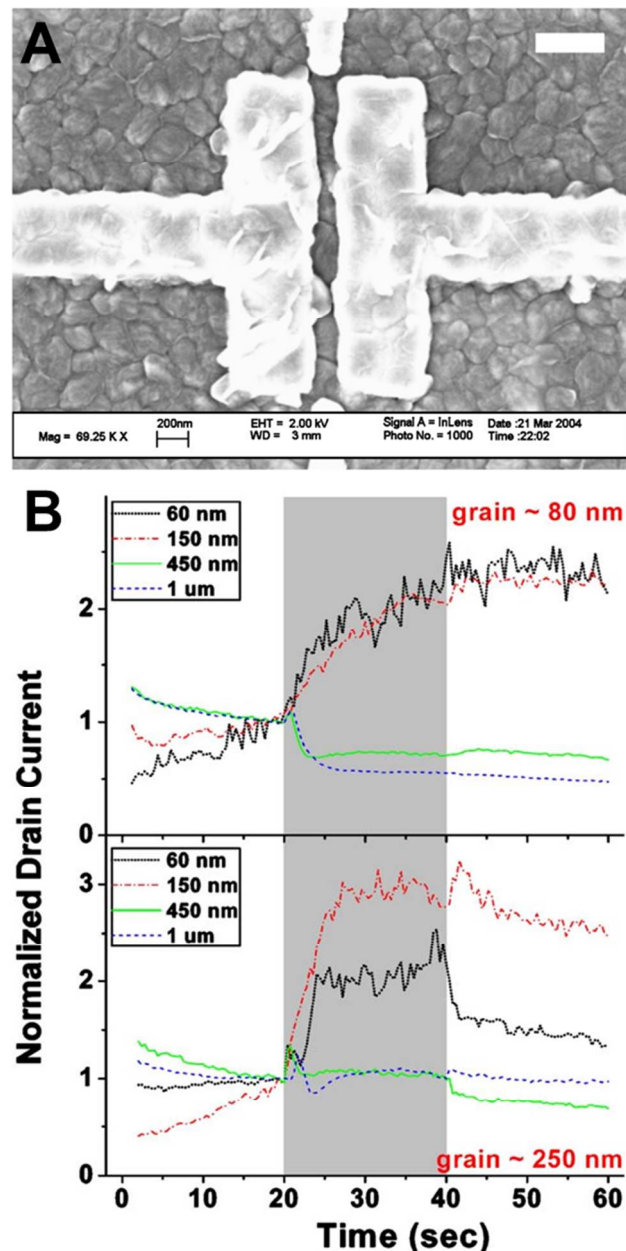


Fig. 3 An example demonstrating the channel length- and grain size-affected sensing mechanism. A): The SEM image of a four-terminal nanoscale pentacene transistor. The observed grains are pentacene. Scale bar = 400 nm. B): Normalized response of I_{DS} of the pentacene transistors of different nanoscale channel lengths and grain sizes towards 1-pentanol dosing. The channel lengths and grain size in each case are presented as inserts. Copyright 2004, AIP Publishing LLC.

In OFET sensors, the surface of OSCs, grain boundaries, dielectric interface, the OSCs/electrode contact interface *etc.*, could be affected by analytes.^{6, 12, 18, 19} The above results suggested that two mechanisms affected the responses of the devices:^{18, 19} one was dominant in long channel devices, arousing decreases in current, and another one was dominant in small channel devices, causing increased current. In the former case, numerous grain boundaries existed within the channel such that

the analytes at the grain boundaries played a dominant role, where they trapped mobile charge carriers and reduced the mobility, leading to decreased I_{DS} . In this case, the sensors are termed as grain boundary limited sensing devices.¹² In the latter case, channel length was close to or even smaller than the grain size such that very few number of grain boundaries existed in the channel. The characteristics of micron scale channels were recovered after reverse bias, while the recovering was not complete in nanoscale devices.¹⁸ This indicated that upon the delivery of analytes, there was a doping effect to the OSC layer, which was more evident in small channel devices. It thus was proposed that the doping effects dominated the sensing process for nanoscale devices, where the excess charges aroused by the analyte-OSC interaction augmented the gate-modulated charges.^{18, 19} The overall sensing response was the result of a combination of the trapping effect at grain boundaries and doping effect to the grains.

On the other hand, there is an alternative in-depth opinion to understand the distinct sensing behaviors of these p -type OSCs based nanoscale OFETs toward polar analytes. It is believed that the polar analytes could interact with the image charges at the metal electrode/OSC interface, leading to a modification of the work function of the metal contacts and an improved carrier injection. The increased injection could be reflected in the increased drain currents, as indicated in Fig 3B. In contrast to long channel devices, which are grain boundary limited, the OFET sensors operated in this regime are termed as injection-limited sensing devices.¹² Actually, besides providing deep insights into sensing mechanisms, a nanoscale device allows one to detect very small amount of analytes. Such detection will be difficult in large-area devices, where the incremental change in response produced by low analyte concentrations is small and may be lost in noise.^{18, 19}

It can be seen that the trapping of the accumulated charge carriers, which could induce a shift in V_{Th} , played a significant role during sensing. Now, an important issue is to pinpoint the localization of the trapped charge carriers. This is considered to be a significant topic, since it might pave the way to optimize the sensitivity of the sensors. Generally, the trapping could be either in the bulk of OSCs or at the OSC/dielectric interface *etc.* However, it is practically a tough task to identify the actual location, since the gate dielectric interface is generally covered by OSCs in the device. Recently, a “semiconductor exfoliation” method was used to meet this formidable challenge.²⁰ Here, OFETs using N,N -dialkylsubstituted-(1,7&1,6)-dicyanoperylene-3,4:9,10-bis(dicarboximide) derivative (Polyera ActivInk™ N1400), an air stable n -type OSC, as active layer, were charged by applying a gate bias under NO_2 ambient. The surface potential within the channel of the devices was subsequently measured. Simply by using adhesive tape, the OSC were then exfoliated from the transistors, giving out uncovered gate dielectric (Fig. 4A), which was accessible for surface potential measurement. It was found that the V_{Th} shifted to the applied gate bias after the devices were charged, implying the trapping of the free charge carriers. More importantly, as shown in Fig. 4B, the surface potentials before and after exfoliation were very close. This indicated that the charges in the NO_2 sensing system were not trapped in the bulk of OSCs but at the gate dielectric interface

(Fig. 4C). This proposal was further confirmed by other two transistors using poly(perylene bisimide acrylate) and polytriarylamine, which are n - and p -type semiconductors, respectively, as active layers. This suggested that nature of the gate dielectrics but not the type of semiconductor is crucial to the charge trapping dynamics in some cases.

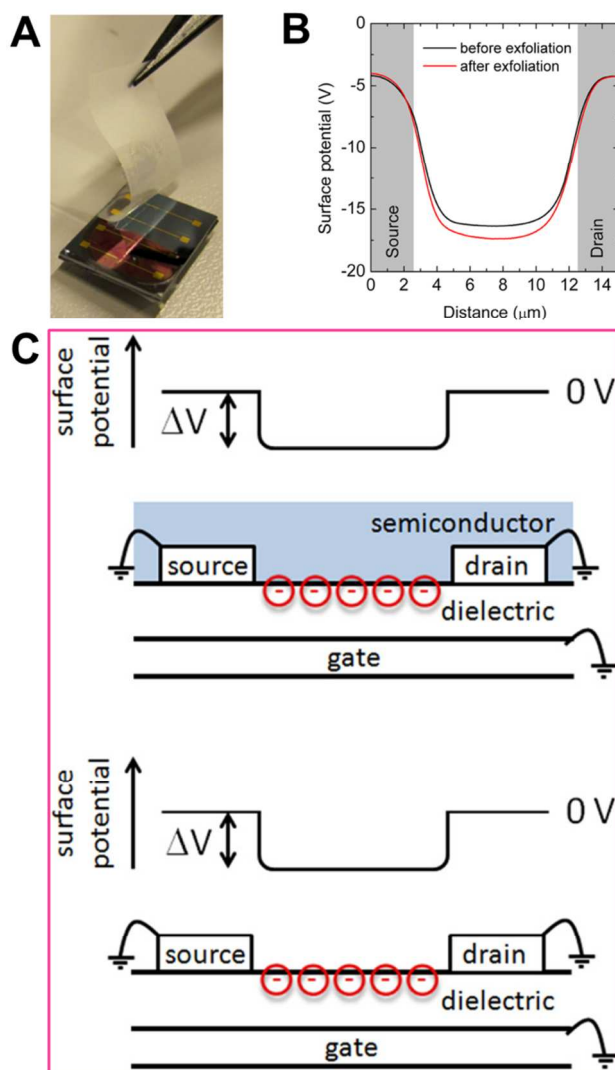


Fig. 4 The localization of the trapped charge carriers in OFETs identified via a “semiconductor exfoliation” method. A): A photo showing the adhesive tape-assisted exfoliation of OSC layer from a Polyera ActivInk™ N1400 transistor. B): The surface potential within the transistor channel before and after the OSC layer exfoliation. C): A schematic illustration of the exfoliation experiment to localize the trapped charge carriers. Top panel: before the exfoliation. Bottom panel: after the exfoliation. Copyright 2012, AIP Publishing LLC.

2.2.2. Indirect responses

In the above examples, OSCs work not only as transistor channel for charge transport but also as responsive layer for sensing. One has to consider both charge transport behavior and sensing capability of OSCs when such sensors are proposed, where an optimization of both sensing and charge transport behaviors of a OSC might be required.²¹ Actually, besides the properties of the employed OSCs, the morphology of the active

layers, the length of the channel *etc.*, an appropriate modification of gate dielectrics, is another important issue that could affect the performance of OFETs.^{2, 5, 10, 22} This could also be harnessed to construct OFET gas sensors in terms of electrochemical or chemical doping of OSCs, or *via* affecting the morphology, hydrophobicity, and the trap density of OSCs.^{23, 24} In these cases, owing to the separation of the sensing mechanism from the

charge-transport functionality of OSCs, the established high-performance OSCs could be employed and synthetic efforts for optimizing both sensing and charge transport capabilities of a OSC might no longer be required.²¹ This might provide new opportunities for OFET gas sensors of different mechanisms.^{21, 23, 24}

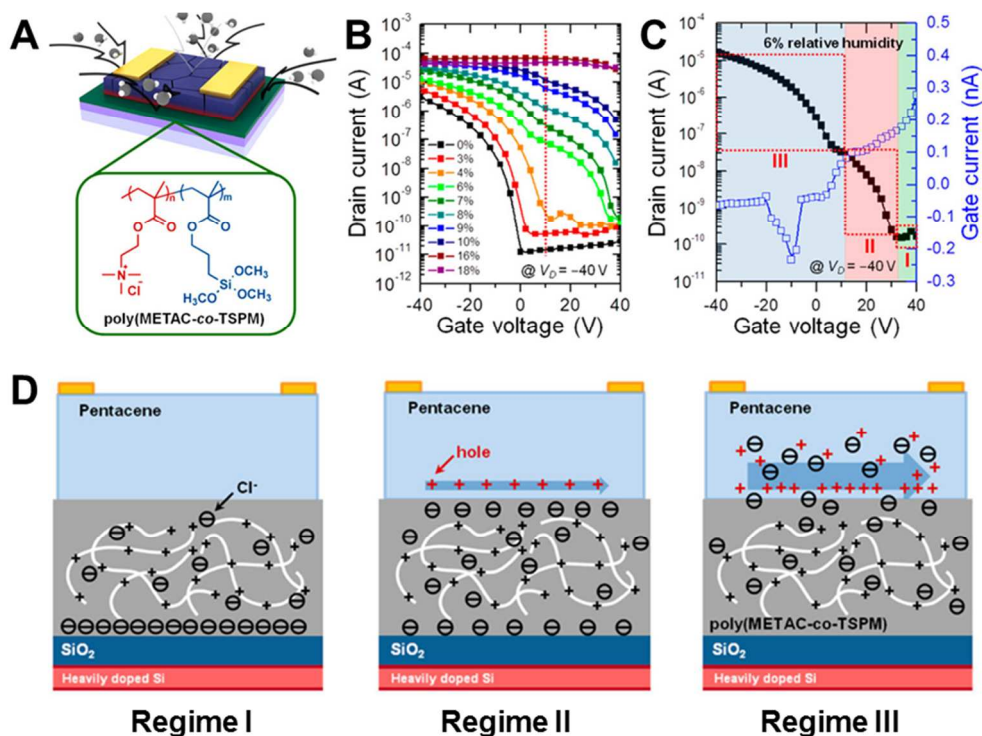


Fig. 5 Sensors of indirect responses in terms of inserting a responsive layer at the OSC/dielectric interface. A): Scheme of the sensor containing an inserted humidity-responsive polyelectrolyte gate dielectric layer, poly(METAC-*co*-TSPM). B): Transfer characteristics of such transistors measured at various humidities. C): A representative transfer characteristic (black) of the device at a relative humidity of 6% plotted with gate current (blue). D): A schematic diagrams of the proposed working principles under different V_{GS} regimes. Copyright 2013, American Chemical Society.

For example, Park *et al* reported that pentacene OFETs-based humidity sensors of ultrahigh sensitivity could be constructed by inserting a humidity-responsive polyelectrolyte layer, poly[2-(methacryloyloxy)ethyltrimethylammonium chloride-*co*-3-(trimethoxysilyl)propyl methacrylate] (poly(METAC-*co*-TSPM)), at the pentacene/SiO₂ interface (Fig. 5A).²³ The overall current level of the as-schemed OFETs displayed a distinct increase as the relative humidity was increased, where a greater increase was observed under positive V_{GS} than under negative V_{GS} values (Fig. 5B). It was found that in response to a 15% change in the relative humidity, the current level of the devices was amplified 7 orders of magnitude.

These results are different from the conventional pentacene OFETs-based humidity sensors, where no moisture-responsive layer was inserted.²⁵ In this case, instead of boosted I_{DS} , the devices with unmodified dielectric layer generally exhibited decreased current output as the relative humidity was increased. This could be a consequence of charge trapping at the grain boundaries of the polycrystalline OSC by polar water molecules. On one hand, H₂O residing at the grain boundaries could interact with hole charge carriers by altering the electric field therein, reducing μ . On the other hand, diffusion of H₂O into grain boundaries might change the intermolecular interactions,

increasing energy barrier for intergrain charge carrier transport. Moreover, ions associated with H₂O might screen the electric fields at the channel and thus lowered the concentration of gate-induced mobile carriers.²⁵ These issues resulted in a degradation of the performances of the devices upon exposure to moisture.

As shown in Fig. 5C, different from those measured under dry conditions, the transfer characteristics of the pentacene OFETs modified by poly(METAC-*co*-TSPM) displayed an inflection point within the ON regime in the presence of humidity (6%).²³ Thus, starting from the regime of the most positive V_{GS} , the performances of the devices under moisture could be divided into three distinct regimes by the inflection point and the turn on voltage. The sensors worked in different mechanisms under different V_{GS} ranges, as illustrated in Fig. 5D. Upon exposure to moisture, Cl⁻ could be released from the polyelectrolyte backbone. Driven by the strong positive gate field, most of the released Cl⁻ migrated to the SiO₂/polyelectrolyte interface when the highest positive V_{GS} values were imposed (Regime I). Accordingly, the Cl⁻ could only influence the hole transport at the pentacene/electrolyte interface slightly such that the transistor remained in OFF state over this regime. In Regime II, where smaller but positive V_{GS} values were applied, some of the Cl⁻ were capable of escaping from the SiO₂/polyelectrolyte interface,

owing to the weaker gate field. The escaped Cl^- were distributed over the polyelectrolyte layer, where those near the pentacene/electrolyte interface contributed to hole formation in the transport channel or to an electrochemical doping of the pentacene. As V_{GS} decreased, a higher number of Cl^- contributed to hole accumulation at the pentacene/polyelectrolyte interface, leading to an increased current. In Regime III, where a negative V_{GS} was applied, instead of being attracted to the

$\text{SiO}_2/\text{polyelectrolyte}$ interface, the Cl^- were pushed to the pentacene/polyelectrolyte interface or even into the pentacene layer *via* grain boundaries. This essentially enhanced the doping process, leading to a sudden increase in the current, where the inflection point occurred. This was confirmed by the observations that gate current (Fig. 5C) exhibited an immediate increase upon entering Regime III.

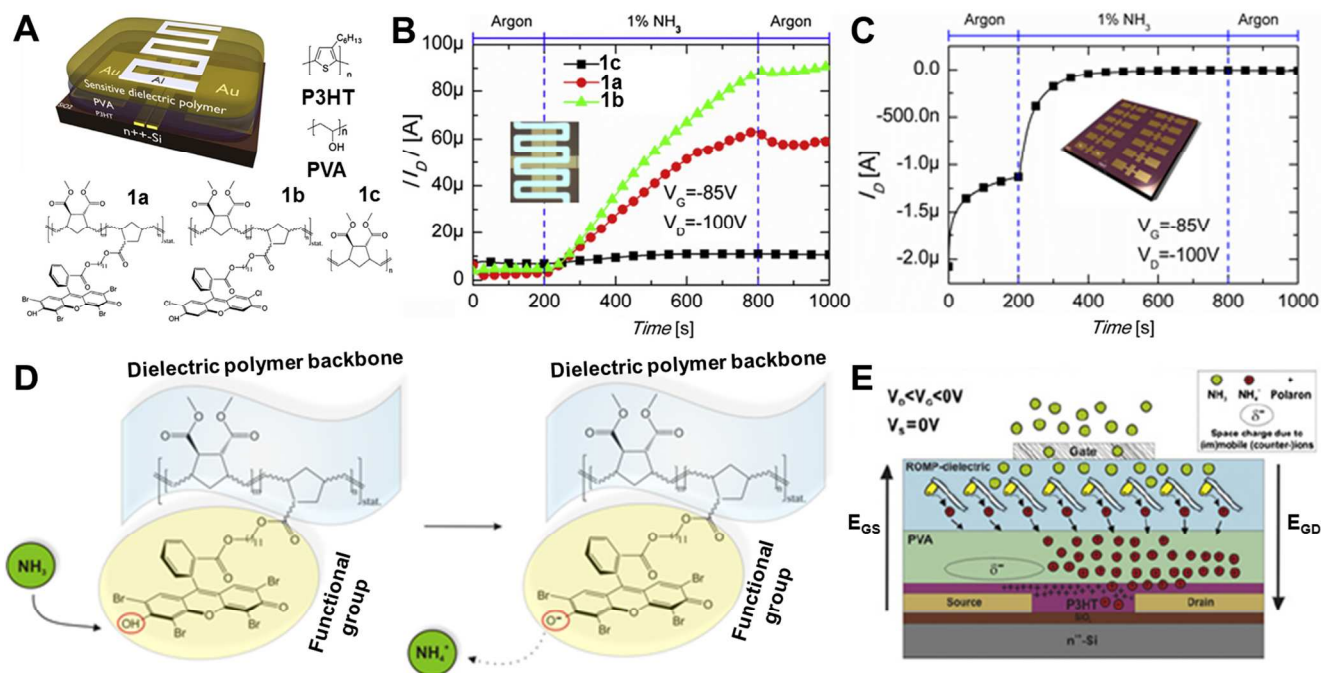


Fig. 6 OFET sensor of indirect responses based on TGBC-structured transistors using sensitive species as gate dielectrics. A): Scheme of the device with a meander-shaped top-gate Al electrode, and the molecular structures of rr-P3HT (active layer), PVA (intermediate layer), pH-sensitive ROMP gate dielectrics (1a, 1b), and the reference gate dielectrics (1c). B): I_{DS} response of such transistors based on various sensitive dielectrics towards NH_3 . The inset shows the top-view image of the device. C): I_{DS} response of the corresponding BGBC-structured OFETs towards NH_3 . The inset depicts the scheme of a sample with 12 devices. D): Scheme of the deprotonation reaction between NH_3 and 1a. E): A schematic depiction of the response mechanism of such sensitive gate dielectrics-based TGBC-structured transistors. Copyright 2012, Elsevier.

According to the position of the electrodes, OFETs could be constructed in several configurations (Scheme 1). Most of the above paradigms are based on bottom-gate structures. Actually, the geometry of the OFETs is an important factor affecting their performances.⁵ This paves alternative avenues for OFET gas sensors of new working principles. By using regioregular poly(3-hexylthiophene) (rr-P3HT) as OSC, pH-sensitive, ring-opening metathesis polymerized (ROMP) materials 1a and 1b (Fig. 6A) as gate dielectrics and 1c as reference material, and polyvinyl alcohol (PVA) as intermediate layer between OSC and gate dielectrics, Klug *et al* reported that bottom-contact OFETs with a meander-shaped top-gate (aluminum) structure (Fig. 6A) could be used for low-concentration NH_3 detection.²¹ Upon exposure to 1% NH_3 , the devices based on reference material 1c could only display slight responses, while I_{DS} exhibited distinct increase in the case of the OFETs using 1a and 1b as gate dielectrics (Fig. 6B). On one hand, the PVA-based devices without an additional ROMP-dielectric did not show any response to NH_3 . On the other hand, different from the devices of a top-gate structure, the corresponding BGBC OFETs displayed distinctly decreased I_{DS} upon NH_3 exposure (Fig. 6C). This result is similar to the observations of the traditional rr-P3HT OFET NH_3 sensors

(bottom-gate configuration without analyte-responsive gate dielectric).²⁶ The reduction of I_{DS} could be ascribed to charge carrier trapping,⁵ since the presence of polar molecules, such as NH_3 , is known to detrimentally affect the charge transport by increasing the amount of energetic disorder through charge-dipole interactions.²⁶

A response mechanism was proposed for these emerging ROMP dielectrics-based (1a and 1b) devices. It was suggested that the NH_4^+ generated by the chemical interactions between NH_3 and the dye-bearing, pH-sensitive groups of the active-sensing ROMP-dielectrics played an important role, as elucidated in Fig. 6D, 6E.²¹ During NH_3 exposure, the OFETs were operated at a potential difference between top-gate and drain electrodes, giving out an electric field E_{GD} , which pointed to the direction of the drain electrode. The mobile NH_4^+ could thus move within the ROMP dielectrics in the direction of the drain electrode and localize near the drain region at the PVA/semiconductor interface or even in the rr-P3HT layer. On the other hand, owing to the presence of an electric field E_{GS} between source and gate electrodes, which pointed into the direction of the gate, the density of the positive ions nearby the source electrode was reduced. Here, immobile/mobile negatively charged ions, for

example, OH^- originating from residual water or ions not fully removed by dialysis of PVA, built up a space charge (δ^-). As a result of the accumulated ions and/or space charge near the interfaces to the electrodes and rr-P3HT, the density of mobile carriers in OSC channel was increased by an electrochemical doping of the contacts (reduced charge injection and ejection barriers between gold and rr-P3HT) and/or the OSC, the formation of electric double layers, the release of trapped charge carriers and/or by space charge polarization of the dielectric. These issues led to the observed sensor responses.

Besides analyte-responsive polyelectrolytes, alkaline gas (such as NH_3) sensors might also be constructed using rr-P3HT OFETs, where organosilanes terminated with sulfonic acid functionalities were inserted at the rr-P3HT/gate oxide interface.²⁴ Upon exposure to analytes, the devices displayed distinct responses with regard to their V_{Th} and I_{DS} . The doping and dedoping processes in close spatial proximity of the conducting channel, which were related to the protonation and deprotonation of rr-P3HT, played an important role.

In most of the above examples, the responses of the OFETs are induced by chemical interactions between the gaseous analytes and the devices, regardless of direct or indirect working principles. Actually, physical/tactile stimulations, for examples, pressure, gas touch, *etc.*, could also bring out responses.⁷ Seo *et al* reported the fabrication of P3HT OFETs, whose top was mounted with liquid crystal (LC) molecules 4-cyano-4'-pentylbiphenyl (5CB).²⁷ Such liquid crystal-on-OFET (LC-on-OFET) displayed substantially enhanced I_{DS} compared to the pristine devices without the LC layer. More fascinatingly, the I_{DS} of the LC-on-OFETs was further increased significantly upon applying a nitrogen flow to the LC layer, even when the gas flow intensity was so low that human skins could not feel at all. Similar perceptive sensation was also achieved using the LC-on-OFET devices with a polymer film skin, indicating the potential applications of such novel devices.

It was suggested that the synergy effect between the collective behavior of LC molecules and charge-sensitive channel layer played an important role for such interesting phenomena (Fig. 7). Originally, owing to the hexyl groups of P3HT, 5CBs in the top layer were basically aligned in a homeotropic geometry with a tilted angle from the vertical axis. When electric fields were applied to turn on the device, most of 5CBs were aligned nearly in the source-to-drain direction parallel to the channel. This was induced by the applied electric fields. Because of the negative values of V_{DS} and V_{GS} (negative electric fields), the negative poles of the 5CBs were headed for the source electrode and tilted toward the surface of P3HT layer (Fig. 7, left). Such alignment of the strong dipole of the LC molecules could in turn induce positive charges in P3HT channel, leading to an evidently enhanced hole current. Finally, such alignment of the LC molecules was significantly reorientated by the nitrogen gas flow touch such that the negative dipole parts of the 5CBs might be much closer to the surface of P3HT layer (Fig. 7, right), inducing additional positive charges in the channel, and rendering further amplified current.

Actually, apart from the above working principles, some other mechanisms could also be responsible for the operation of OFET gas sensors. Some of them will be mentioned concisely in the

following paragraphs. For more mechanisms, interested readers are suggested to consult other earlier review articles,^{6, 11} although brief discussions were presented therein.

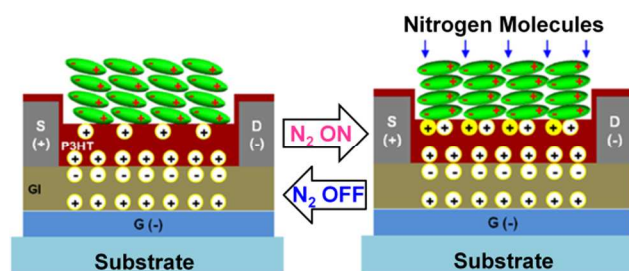


Fig. 7 Gas touch induced responses of a LC-on-OFET, where a 5CB LC layer works as sensitive layer, and P3HT serves as active layer. The synergy effect between the collective behavior of LC molecules and charge-sensitive channel layer plays an important role during the sensing. Copyright 2013, Macmillan Publishers Limited.

3. Protocols for high-quality OFET gas sensors

It can be seen that although OFETs are simply three-terminal electronics, complex and multiple mechanisms are responsible for their responses to external stimuli. This is owing to the fertile diversity of the selectable OSCs and dielectric materials, the existence of various modulatable interfaces, and the variety of device configurations *etc.* On one hand, it is currently an importance subject to shed deep insights into the underlying mechanisms. On the other hand, a good understanding on the mechanisms might provide new opportunities for high-quality OFET gas sensors.

From the structure and operation points of view, OFETs could be considered to be two-terminal organic chemiresistors when no gate voltage is applied. In contrast to the two-end organic chemiresistors, one of the most distinguished advantages of the use of OFETs is their intrinsic capability to modulate the electric performances with a gate bias. This renders OFETs multi-parameter electronics,^{13, 28, 29} where a number of parameters, such as μ , V_{Th} , I_{DS} , $I_{\text{on}}/I_{\text{off}}$ *etc.*, could be separately but readily extracted. Together with the considerable variety of the OSCs, this renders OFETs promising platform for electronic nose.^{13, 28} Indeed, compared to the organic chemiresistors, OFETs are structurally and operationally more complex, the formation of a charge accumulation layer at the insulator/OSC interface, which is induced by a V_{GS} , however, enables the use of ultrathin films or nanostructured materials as the active layers of OFETs. On one hand, this gate-induced amplifying effect makes OFETs more scalable and sensitive. In other words, the OFETs could actually be considered to be 'amplified chemiresistor'.²⁹ On the other hand, the use of ultrathin films or nanoarchitected OSCs favors a rapid capture, diffusion, and release of the analytes, facilitating miniature yet high-performance sensors of expeditious response/recovery, which are substantially desired for uses.

The development of OFETs with high μ , large $I_{\text{on}}/I_{\text{off}}$, and low V_{Th} *etc.*, occupies an important position in OFETs' history. Numerous OSCs have thus far been developed aiming at high μ , but not sensitivity.²⁹ In contrast, gas sensors using OFETs as transducers primarily emphasize the analyte-induced changes in their electrical performances. This makes it possible that the established OSCs of high or even moderate charge transport

capabilities might be useful for high-quality OFET gas sensors.²⁹ Several issues, including high selectivity and sensitivity, good stability and durability, response/recovery time, fast multiparameter data acquisition and so on, are strongly desired by high-quality gas sensor. In this section, the state-of-the-art protocols for high-quality OFET gas sensors will be presented.

3.1. Molecular Modification towards OSCs

Commonly, OSCs of high electrical performances are based on simple polyaromatic structures and do not possess reactive sites that promote specific sensory response.³⁰ This disfavors OFET sensors of high sensitivity, specificity and selectivity *etc.* Molecular engineering in terms of design of emerging OSCs, and the launch of new dielectrics with specific functionalities, namely, the implantation of certain recognition, receptor or reactive sensing sites *via* covalent or noncovalent bonds to the device, is among the most frequently employed protocols to meet this issue. Thanks to the great advances in molecular engineering, numerous OFET gas sensors of bright application possibilities have been developed.

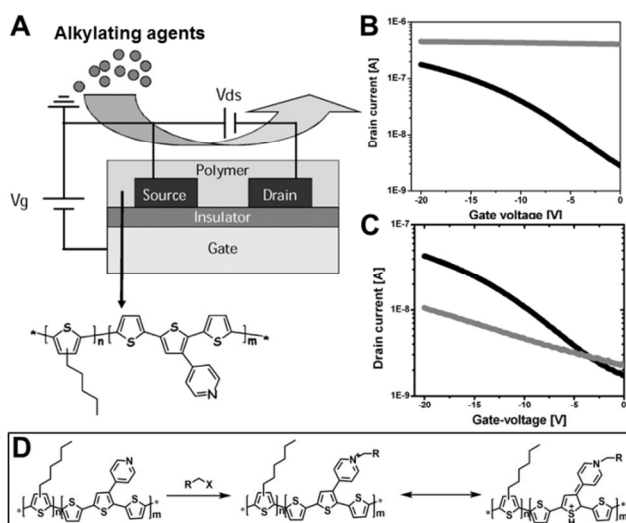


Fig. 8 Sensing responses induced by the formation of covalent bonds between analytes and OSC. A): The scheme of the transistor and the molecular structure of the *ad-hoc*-designed polythiophene copolymer functionalized with pendant pyridine groups. B and C): Transfer characteristics of the transistors measured before (black) and after (gray) exposure to an alkylating agent, methyl iodide (B), and to a non-reactive analyte, methanol (C). D): A scheme illustrating the doping mechanism induced by the formation of covalent bonds. Copyright 2010, Wiley.

As one of the most important OSCs, tetrathiafulvalene (TTF) has received much attention as sensing materials. This is owing to their built-in strong electron-donating properties, rendering them easily susceptible to electron acceptors. However, this in turn leads to an easy doping of their films by oxygen, giving out high off-state conductivity and thus disfavoring their uses as highly sensitive OFET sensors. To address this disadvantage, Yang *et al* designed and synthesized a TTF derivative benzothiadiazole-tetrathiafulvalene (BTDA-TTF) and investigated their sensing behaviors.³¹ BTDA group was introduced as an electron-withdrawing group to lower the electron-donating ability of TTF moiety. As expected, the BTDA-TTF OFETs displayed low I_{off}

and high $I_{\text{on}}/I_{\text{off}}$ compared to the transistors based on other TTFs. The performances of the devices exhibited only slight changes upon exposure to air, indicating their good stability toward oxygen.

In contrast, evident increases in I_{off} were observed after exposure to diethyl chlorophosphate (DECP) or POCl_3 vapor. When the vapor concentration was lower than 100 ppm, I_{off} was enhanced gradually by increasing the vapor concentration, where vapors with concentrations as low as 10 ppb could be effectively detected, suggesting the realization of a high sensitivity. The oxidation of BTDA-TTF in the presence of DECP and POCl_3 , which could result in the generation of more hole carriers, together with other factors like film morphology, were suggested to be responsible for these results. On the other hand, the μ of the device was reduced upon exposure to DECP or POCl_3 vapor of a concentration higher than 100 ppm. Diffusion of these analytes into the OSC layer, which would trap the carriers, contributed much to the reduced μ . Interestingly, when 2,4,6-trinitrotoluene (TNT) vapor of 100 ppb was sensed, the I_{off} remained almost unaltered, while the μ and saturation current were reduced. It was proposed that that TNT might not induce the formation of more hole carriers, but it might trap the carriers and slowed down the movements of carriers, resulted in a reduction in μ and saturation current. This investigation suggests that an appropriate modification to OSCs might lead to different sensing mechanism, affording opportunities for OFETs sensor of high sensitivity, although the selectivity still needs to be improved by an introduction of receptors of specific recognition capability.

The noncovalent interactions between analytes and devices play an important role for the responses of most of the existing OFET gas sensors. Actually, covalent interactions, *viz.*, the formation of covalent bonds between the analytes and the OSCs, could also contribute much to the responses, facilitating gas sensors of potential uses in some special cases. Gannot *et al* reported the synthesis of a novel polythiophene copolymer functionalized with pendant pyridine groups and investigated the response of its OFETs to vaporous alkylating agents (Fig. 8A),³² which are significant chemicals in organic synthesis, medicine, agriculture and even chemical warfare. Such OFETs displayed standard electrical characteristics when no analytes were exposed. Interestingly, upon exposure to alkylators, such as methyl iodide, chloromethoxy ethane, 1-chloro-2-ethylsulfanyl ethane, and benzyl bromide *etc.*, the devices showed considerably higher currents with its channel became conductive, from which a resistor-like response without the gate-induced amplifying effect was observed (Fig. 8B). This was different from the results obtained when the traditional P3HT OFETs were used as transducer, or when non-reactive gases, such as alcohols and acetone *etc.*, were used as analytes, wherein only deteriorations of the electrical characteristics could be observed (Fig. 8C). Such responses towards the alkylating agents were suggested to be owing to the covalent alkylation/quaternization of the pyridine units of the polythiophene copolymer (Fig. 8D), resulted in the formation of electron-deficient pyridinium groups, which attracted charge density from polythiophene skeleton, leading to a high-level *p*-type doping and the loss of the gate effect.

In the above sophisticated examples, functional sensing sites are covalently grafted onto OSCs to induce selective and

sensitive responses to target analytes. Nevertheless, when this strategy is addressed, an optimization of the functional groups and the electrical performances of the employed OSCs should generally be taken into account to achieve an acceptable level of sensor performances. This is owing to the fact that the presence of functional substituents on OSCs might induce changes to its morphology, solubility, and device performances.⁷ An efficient strategy to overcome this problem is the use of blends of OSCs of high electrical performances and sensing molecules of specific recognition capacity.

As known, owing to the specific interactions between boron atoms and lone pairs, boranes could work as excellent complexation agents for Lewis bases. By taking the advantage of this inherent feature, Huang *et al* reported that transistors based on mixture of tris-(pentafluorophenyl)borane (TPFB) and CuPc or TPFB and cobalt phthalocyanine (CoPc) could display essentially improved sensitivity towards NH₃ compared to those based on pure CuPc or CoPc, where the limit of detection (LOD)

was conservatively estimated to be as low as 0.35 ppm.³³ Such high-performance NH₃ sensors, using TPFB as additive, could also display distinct selectivity towards NH₃ compared to other organic vapors, such as methanol, acetone, ethyl acetate, dichloromethane, hydrogen, *etc.*, although very high concentrations of these analytes were used. On the other hand, when triphenylmethane (TPM) or triphenylborane (TFB), whose molecular structures were similar as TPFB, was used as additive, no obvious improvement in sensitivity could be realized. More interestingly, the electronic responses of such sensors could be memorized by storing the devices in a sealed container at a low temperature. This quality is of significance in the cases that the reading of the device right after the exposure is impractical, permitting *ex situ* sensing uses in some special cases. The cooperative host-guest interactions between TPFB and NH₃ in terms of the strong B–N coordination interaction and hydrogen bonds played an important role for the high-quality of the TPFB involved devices.

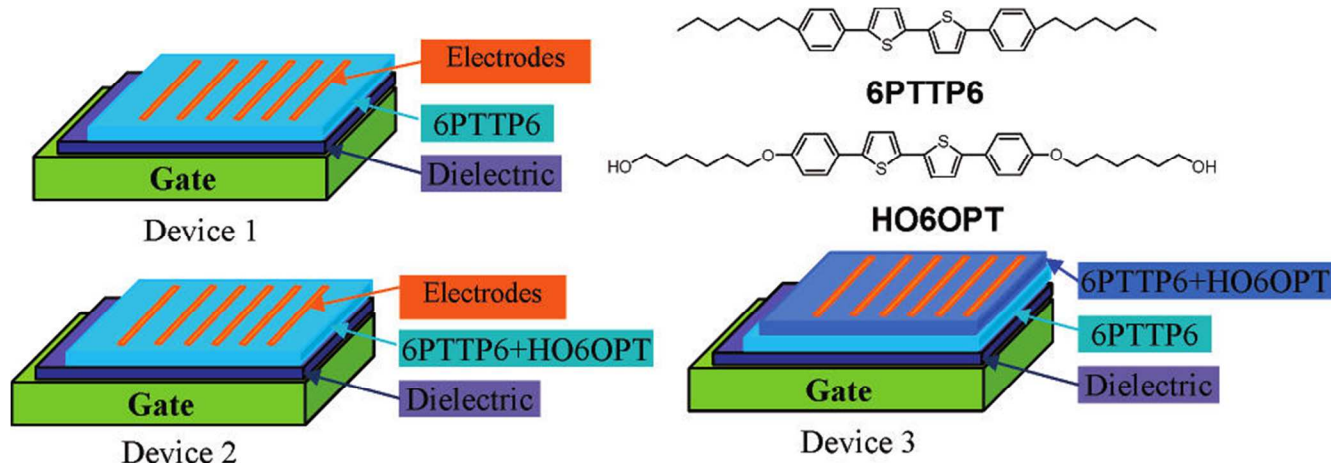


Fig. 9 OFET sensors of high selectivity realized via a sensory layer implantation protocol. The figure shows the molecular structures of the phenylene-thiophene tetramers substituted without (6PTTP6) and with (HO6OPT) hydroxyl functional groups, and the schematic illustration of various transistor structures. Owing to a combination of the advantages of the high electrical performance of the inner 6PTTP6 charge transport layer, and the reorganization capability of the outer sensing layer, the two-layer heterostructured Device 3 exhibit nice selectivity towards DMMP. Copyright 2007, American Chemical Society.

3.2. Sensory layer implantation

The above example elucidates that incorporation of additive molecules of specific sensing capability to OSCs of high electrical performances could indeed lead to high-quality OFET gas sensors, where the tedious synthesis works for OSCs bearing specific sensing groups could be avoided. However, it is, to a great extent, difficult for this effective method to work as a general strategy, since the molecular stacking and morphology of the channel materials, which might affect the performance of the devices, could always be altered when additive molecules are presented. On another front, in terms of the thickness-independent electrical performances of OFETs, it is widely verified that the gate-field-induced charge accumulation and transport are mostly confined in the first several nanometers or a few layers of the channel film nearby the OSCs/dielectric interface.³⁴ This means that the implantation of an additional sensory layer on the top of an OFET might induce selectivity and sensitivity to the OFETs while the inherent high electrical

performances of the device might be preserved.^{34, 35}

With regard to this strategy, a representative example was presented by Huang *et al*, where they reported the synthesis of phenylene-thiophene tetramers, 5,5'-bis(4-*n*-hexyl-phenyl)-2,2'-bithiophene (6PTTP6) and 5,5'-bis(4-hydroxyhexyloxyphenyl)-2,2'-bithiophene (HO6OPT), which were substituted without and with hydroxyl groups, respectively (Fig. 9).³⁵ Three kinds of devices, *viz.*, single layer OFETs based on pure 6PTTP6 (Device 1) and blend of 6PTTP6 and HO6OPT (Device 2), and two layer devices based on a 6PTTP6 bottom layer and a 6PTTP6-HO6OPT blend top layer (Device 3), were fabricated, and their responses towards vaporous DMMP were investigated. The saturation I_{DS} of the nonfunctionalized Device 1 and functionalized Device 2 decreased dramatically upon exposure to DMMP, where obvious V_{GS} -dependent responses were observed. However, compared to Device 2, Device 1 displayed a much longer response time, whereas the saturation current of Device 2 was 1 order of magnitude lower comparatively, making them not suitable for sensor uses. In contrast, the two-layer heterostructured Device 3 displayed a comparable response time

with Device 2, and a similar magnitude of I_{DS} variation as Device 1, indicating fast yet sensitive responses. More significantly, Device 3 exhibited evident selectivity towards DMMP compared to the interference analytes, such as 2-octanone, butyl butyrate, and acetic acid, *etc.*

The high sensing performance of the heterostructured Device 3 was suggested to be owing to a combination of the advantages of the high electrical performance of the inner 6PTTP6 layer, and the reorganization capability of the outer blend layer, where the former served as charge transport layer, whilst the latter provide a distribution of OH groups as receptor sites. Here, the OH group of HO6OPT formed hydrogen bonds with DMMP, leading to increased adsorption and electronic effects. The excellent responses of the heterostructured device could be owing to the electric fields induced by the polar DMMPs, whose magnitude was comparable to the transverse source-gate field and was much larger than the longitudinal source-drain field. This suggested that the dipoles of DMMPs were capable of trapping mobile charges and significantly decreased current by changing both the V_{Th} and μ .

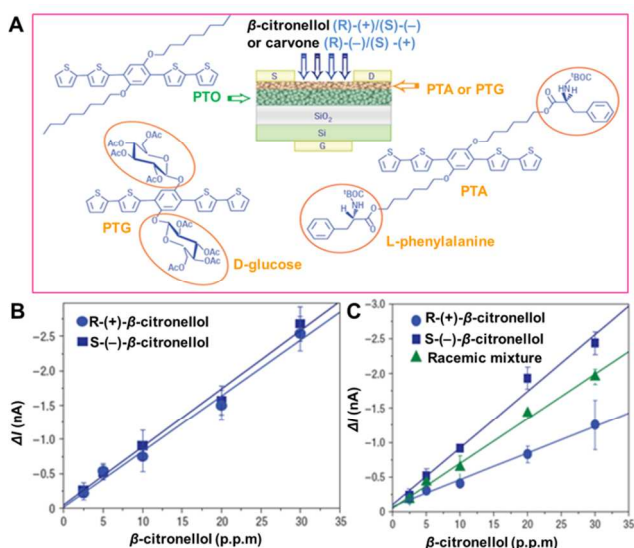


Fig. 10 OFET-based chiral gas sensor by means of implanting an enantioselective recognition sensory layer. Chiral pairs-dependent selectivity could be realized by taking the advantage of chiral recognition between chiral sensory layer and chiral analytes. A): The scheme of the bilayer OFET chiral sensor, and the molecular structures of the involved achiral (PTO) and chiral (PTA and PTG) oligomers. B): The response of the achiral single-layer PTO transistor towards (S)-(-)- β -citronellol and (R)-(+)- β -citronellol as a function of analyte concentration. C): The response of the chiral bilayer transistor towards (S)-(-)- β -citronellol, (R)-(+)- β -citronellol, and their racemic mixture as a function of analyte concentration. Copyright 2008, Macmillan Publishers Limited.

Owing to the intrinsic significance of chirality in biochemistry, life sciences, and medicinal chemistry *etc.*, sensors capable of chiral discrimination have been attracting great attention. However, enantiomeric recognition *via* OFETs is still a tough task encountered by scientists. This is owing to the fact that the two enantiomers have mirrored geometries. Consequently, they could only behave differently in chiral circumstances, namely, only when they interact with other chiral species. To address this formidable challenge, Torsi *et al* reported that gas sensor capable of differentially detecting optical isomers could be constructed

via a bilayered OFET.³⁴ The OFETs (Fig. 10A) were composed of an achiral phenylene-thiophene oligomer (PTO) inner layer, and a chiral outer layer, which is a film of phenylene-thiophene oligomers bearing L-phenylalanine amino acid groups (PTA) or β -D-glucosidic units (PTG).

The devices based on single-layer achiral PTO displayed nearly similar responses upon exposure to gaseous (S)-(-)- β -citronellol and (R)-(+)- β -citronellol (Fig. 10B). In contrast, the responses of the PTO-PTA bilayer OFETs toward these β -citronellol optical isomers exhibited evident differences, where the sensitivity for the racemic mixture fell right between the two enantiomers (Fig. 10C). Roughly similar results were obtained when the PTO-PTG bilayer OFETs were used to sense the gaseous ketone enantiomers, (S)-(+)- and (R)-(-)-carvone. However, no chiral differential detection could be realized when the PTO-PTA and PTO-PTG OFETs were employed to detect the carvone and citronellol enantiomers, respectively. Such chiral pairs-dependent selectivity was suggested to be owing to the weak intermolecular interactions, which were responsible for chiral discrimination and substantially depended on structural differences of the involved chiral molecules. By taking the advantage of this feature, the recognition capabilities of these chiral gas sensors might be improved in terms of a sensing array. It was suggested that the achiral PTO inner layer worked as charge transport channel, while the chiral outer layer played a role of enantioselective recognition, where the different partition coefficients of the two enantiomers between the outer chiral layer and vapour phase contributed much to the observed selectivity.

Calixarenes, which are phenol-formaldehyde cyclic oligomers, have been attracting great interest in the interdisciplinary fields of supramolecular chemistry and sensor science. This is promoted by their well-understood cavitory geometry and their tunable physicochemical properties, which endow them with unique inclusion capacities *via* host-guest molecular recognition, favoring the construction of sensing systems of high sensitivity and selectivity. Bearing these basic understandings in mind, Sokolov *et al* demonstrated that the pristine OFETs based on 5,5-bis-(7-dodecyl-9H-fluoren-2-yl)-2,20-bithiophene (DDFTTF) could only display poor sensitivity and selectivity towards vaporous analytes.³⁰ Significantly, upon incorporating calixarene container molecules, such as calix[8]arene (C[8]A) or C-methylcalix[4]resorcinarene (CM[4]RA), on the top of the devices (Fig. 11A), both the sensitivity and selectivity of the formulated two layer OFETs were substantially enhanced. The C[8]A layer modified devices exhibited a preferential selectivity toward ethyl acetate, whereas those covered by a CM[4]RA sensory layer displayed a perceptive selectivity towards isopropanol (Fig. 11B). Considering the facile availability of various container molecules of different cavity shape, size and physicochemical properties, this effective strategy might be generalized, and will have broad application opportunities for OFET gas sensor of high sensitivity and selectivity, where shape discrimination between gaseous analytes might be realized. Note that, instead of I_{DS} changes, which were frequently used as the sensing readout, the response of such OFETs was measured as the change in the rate of I_{DS} (dI_{DS}/dt). This could avoid the additional error introduced by gate-bias stress, and more importantly, the derivative plot indicated that the devices

exhibited a fast rate of current change that quickly saturated within the initial seconds of analyte exposure. Besides selectivity and sensitivity *etc.*, such an expeditious response is another basic quality strongly desired by high-performance gas sensors.

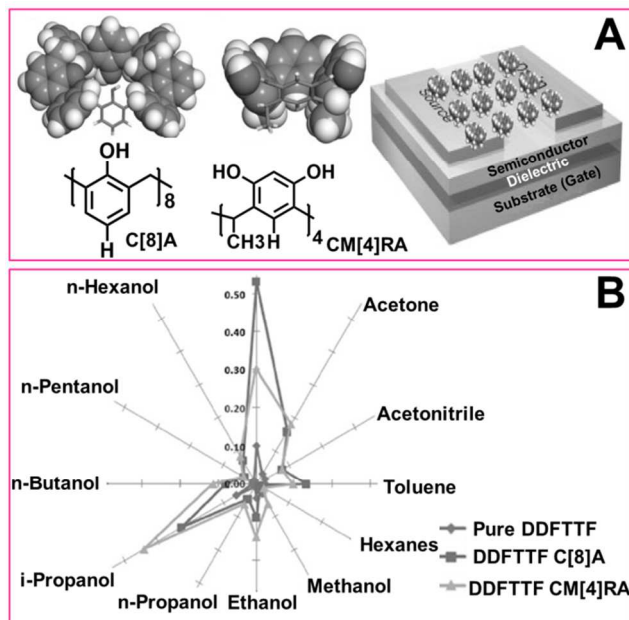


Fig. 11 High-quality OFET gas sensors by means of incorporating a sensory layer of container molecules of tunable cavity. By taking the advantage of the unique inclusion capacities of the container molecules in terms of host-guest molecular recognition, sensors of high sensitivity, selectivity, expeditious responses, and even capable of shape discrimination might be constructed. A): Structures of the calixarene container molecules C[8]A and CM[4]RA, and the scheme of the bilayer DDFTTF OFETs. B): A radial graph showing the enhancement of the calixarene-modified transistors in response to a series of volatile analytes. Copyright 2010, Wiley.

Besides the *ad-hoc*-synthesized sensory molecules, biomolecules of specific biorecognition capacities could also be integrated as a sensory layer into two-layer OFETs aiming at bioelectronic sensors of high sensitivity and selectivity. Angione *et al* reported the construction of functional biointerlayer OFETs (FBI-OFETs), where P3HT was employed as OSC, and functional biosystems, *viz.*, a phospholipid (PL) bilayer, a purple membrane (PM, which was constituted of a PL bilayer including the sole bacteriorhodopsin (bR) protein) film, or a streptavidin (SA) protein layer, were embedded between gate dielectric and OSC (Fig. 12A).³⁶ These FBI-OFETs exhibited excellent sensing capacity towards biorecognition events. For example, the bare P3HT OFETs without functional biolayers could only display slight responses towards volatile anesthetics, such as halothane and diethylether. In contrast, when the PL or PM FBI-OFETs were used, the I_{DS} of the devices showed evident decreases and increases, respectively (Fig. 12B and 12C), while other organic vapors, such as acetone, aroused a much lower response. For PL FBI-OFETs, the decreased I_{DS} was attributed to the anesthetics induced disorder at PL/P3HT interface, generating defects at the field-induced transport interface, thus lowering the current. Here, the I_{DS} alterations displayed a dependence on anesthetic concentration, which spanned the clinical relevant range (Fig. 12D). Such electronic sensing, being particularly sensitive to

subtle changes in the PL membrane, was believed to be a useful tool to deepen the understanding of the anesthesia action mechanism. For PM FBI-OFETs, the increased I_{DS} was ascribed to the anesthetic molecules induced pK_a changes in bR, provoking a proton release, which could be injected into the P3HT layer by gate field. This significant investigation indicated that the use of bioactive molecules as the sensory layer of OFETs might not only favor the construction of extremely performing biosensors, but also could shed deep insights into biologically relevant phenomena, such as membrane weak interfacial modifications.

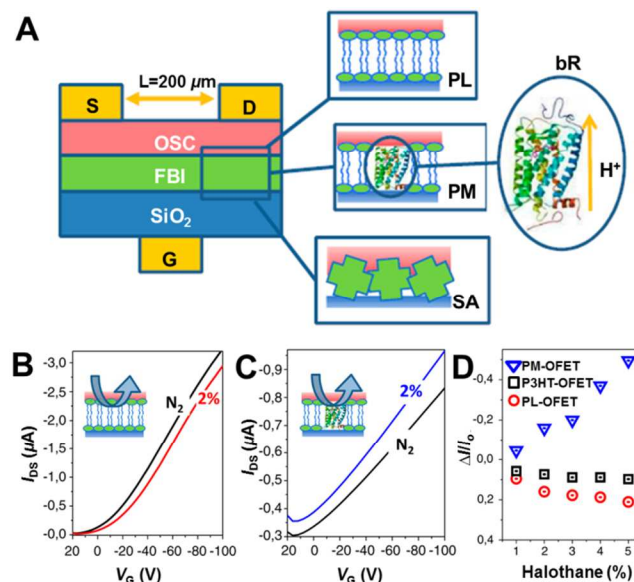


Fig. 12 A representative example showing that bioelectronic gas sensors of high sensitivity and selectivity could be constructed by implanting a biosensing layer of specific biorecognition capacities. A): Scheme of the functional biointerlayer P3HT transistor, and the sketches of the three different FBI structures. B and C): Halothane responses of PL (B) and PM (C) FBI-OFETs. D): PM FBI-OFET (blue), P3HT-OFET (black) and PL FBI-OFET (red) responses to clinically relevant halothane concentrations. Copyright 2012, National Academy of Science.

3.3. Device operating conditions

The performance of OFETs could be affected by V_{GS} . This issue could actually also be harnessed for qualified OFET sensors.^{34, 37} Such gate effects embody the advantages of OFET sensors compared to chemiresistors. For example, it was reported that the responses of rr-P3HT OFETs, where the rr-P3HTs formed a highly ordered nanofibril structure, depended substantially on V_{GS} .³⁷ The I_{DS} decreased at all V_{GS} upon exposure to acetone, where higher V_{GS} favored higher responses, whereas in the cases of toluene, absolutely opposite results were obtained (Fig. 13A). Fascinatingly, the device displayed a positive response at 0 V_{GS} upon exposure to butanol, which however, went from positive to negative with increasing V_{GS} . Significantly, such impressive V_{GS} -affected responses could be used to establish a recognition map towards a series of vaporous analytes of different polarities or even distinct alkyl chains (Fig. 13B), indicating their bright future for molecule discrimination uses. These results are different from most of the above examples such that positive and negative responses could be observed for the

same analyte, indicating the competition of multiple mechanisms, which were determined by the testing parameters such as target analyte and more significantly the electrical operating conditions. The specific sensing mechanisms under the certain parameters were basically synergistic results of intragrain and grain boundary effects, which produced positive and negative responses, respectively.

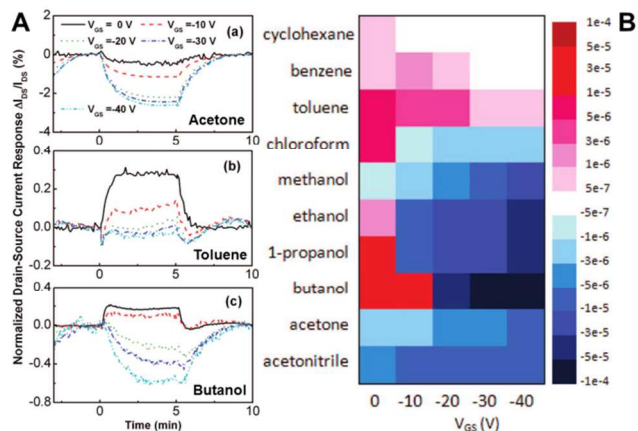


Fig. 13 A typical scenario demonstrating that the performance of OFET gas sensors could be dramatically affected by device electrical operating conditions in terms of V_{GS} -affected responses. A): V_{GS} -determined temporal responses of nanostructured rr-P3HT transistors towards acetone (top), toluene (middle), and butanol (bottom) vapors. B): A contour map illustrating the effect of applied V_{GS} on OFET I_{DS} responses towards 10 vaporous analytes. The establishment of the recognition map indicates the bright future of such electrical operating condition-affected OFET gas sensors for molecule discrimination uses. Copyright 2008, American Chemical Society.

Commonly, many OFETs suffer from I_{DS} drifts upon prolonged V_{GS} application. This is attributed to a shift in V_{th} driven by continuous static gate bias, and is known as the so-called bias stress effect (BSE). One of the frequently mentioned issues responsible for this bias stress instability is charge trapping of mobile carriers, which possibly occurs at various sites of the OFETs, including OSC/dielectric interface, OSC film, insulator layer *etc.* Although the BSE mechanisms are still not fully clarified, this undesirable electrical instability limits the application of OFETs, especially when they work as sensors, since the resulted baseline instability during the operation of the sensors might interfere with the analyte-induced responses. This might lead to a degradation in sensitivity and make the sensing unreliable. To overcome this unwanted effect, a pulsed gating method, wherein the V_{GS} was switched on and off at a constant frequency during the electrical performances, was developed by Yang *et al* to enhance the baseline stability of phthalocyanine (Pc) OFET gas sensors.³⁸ Under static gate bias, a nonlinear baseline with an average degradation rate of 2.5%/h was observed in CuPc OFETs during exposure to methanol dosing pulses. This is owing to the BSE. Interestingly, by pulsing V_{GS} at 0.1 Hz with a 1% duty cycle, the baseline drift was nearly 28 times reduced to 0.09%/h. By virtue of this pulsed gating method, the uncertainty in chemical sensing was reduced by an order of magnitude. This strategy was applicable to the sensing behaviors of other Pc OFETs towards to other gaseous species, such as organophosphonate nerve agent simulants, indicating its general utility. This unique yet simple method paves an efficient way to

reduce BSE, enhance the operational stability and prolong the lifetime of OFETs, which are important issues required by high-quality sensors.

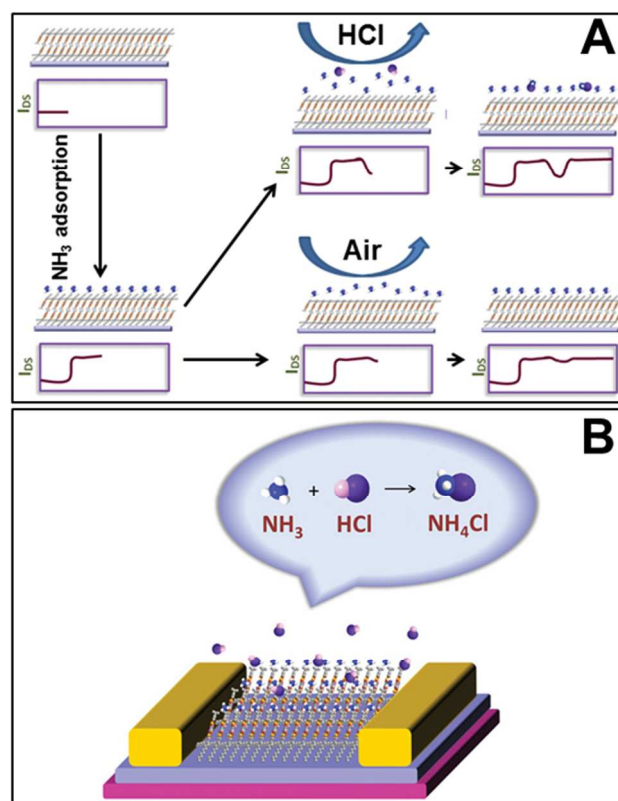


Fig. 14 OFET gas sensors in terms of device operating conditions, where gas-phase chemical reactions are used to promote sensitivity, reproducibility, selectivity and stability. A): Cartoon diagram of sensing process of chemical reaction assisted gas sensor based on NDI(2OD)(4tBuPh)-DTYM2 transistors. B): Schematic diagram of the device structure and sensing mechanism proposed for such gas-phase reaction assisted detection. Copyright 2014, Wiley.

Besides device electrical operating conditions, chemical reactions occurred during the sensing could also promote the transducing with unexpected results. A recent example is launched by Zang *et al.*¹⁴ They found that the responses of NDI(2OD)(4tBuPh)-DTYM2 (n-type OSC) and pentacene (p-type OSC) OFETs towards NH_3 , which displayed opposite changes in I_{DS} , were unrecoverable. Surprisingly, a nice sensitivity, reproducibility, selectivity and stability could be endowed to NDI(2OD)(4tBuPh)-DTYM2 devices absorbed with NH_3 upon exposure to HCl (Fig. 14A). It was suggested that the chemical reaction between NH_3 and HCl contributed much to these interesting results (Fig. 14B), where the original doping aroused by NH_3 was reduced upon the chemical reaction. This proposal could be further verified by pentacene OFETs, where the chemical reaction between NH_3 and HCl also played an important role. The authors called this strategy as “gas-phase reaction assisted detection”. This new approach, a combination of effective chemical adsorption and chemical reaction occurred on OFET sensors, can serve as a shortcut to achieve predictable sensors using well reported OFETs and simple textbook reactions without additional complex molecular design and modification.

3.4. Device structure

While OFETs could generally be constructed in terms of four typical architectures (Scheme 1), the efforts to tune their fine structures might also provide opportunities for high-quality gas sensors. Thus far, most of the dielectric layers of OFET gas sensors are solid species, where the charge carrier transport functionality of OSC occurs mainly in a few molecular layers at OSC/dielectric interface. Not all the gas analytes could reach the response sites during the sensing, limiting the sensitivity and resolution capacity of the sensors. To address this issue, Shaymurat *et al* designed a novel gas dielectric OFET for SO₂ detection. The proposed device was based on a gas dielectric structure with a CuPc single crystalline nanowire suspended between source and drain electrodes (Fig. 15A).²² Compared to the corresponding traditional solid dielectric OFETs (Fig. 15B) using poly (methyl methacrylate) (PMMA) as dielectrics, such fascinating gas dielectric OFETs displayed substantially enhanced sensitivity towards SO₂ (Fig. 15C). The LOD was one order of magnitude (from 10 to 0.5 ppm) decreased when the device was changed from solid to gas dielectric. The totally accessed conductive channel of the gas dielectric OFETs, which facilitated direct analyte-OSC interactions, was suggested to be responsible for the improvement of the sensing performances. Considering the gaseous state of the analytes of gas sensors, this novel gas dielectric OFET opened up new ideal for high-quality OFET gas sensors.

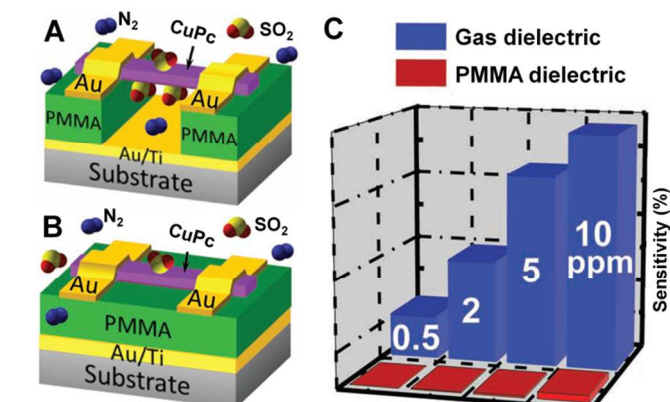


Fig. 15 An emerging example showing that high-quality gas sensors of enhanced sensitivity could be obtained by tuning the fine structures of OFETs. A and B): The scheme of the gas (A) and PMMA (B) dielectric OFET sensors based on individual CuPc single crystalline nanowire. C): Comparison of the sensitivity of gas (blue) and PMMA (red) dielectric transistors in response to SO₂ of different concentrations. Copyright 2013, Wiley.

Devices capable of digital and intelligent readouts are important issues required by modern electronics. It is widely known in the field of digital circuits, the simple electronic inverter in terms of complementary metal oxide-semiconductor (CMOS)-type structure is the most fundamental to realize a conversion from analog to digital signals. Thus far, the most existing OFET gas sensors are performed with an analog signal readout. Therefore, smart sensors capable of a digital readout are absolutely desired for further logic operations and usable products. To conquer this subject, higher order logic circuits utilizing OFETs sensitive to amine vapors are presented by

Tremblay *et al.*³⁹ The device (Fig. 16) was built up by a combination of a *p*- and an *n*-type OSC of matching μ and V_{Th} . By taking the advantage of the additive effect of the synergistic responses of the increased *p*-channel V_{Th} and decreased *n*-channel V_{Th} , the inverter switching voltage shifted to lower voltage when increasing the concentration of amine, giving out the unambiguous 1 or 0 readouts. This kind of signal in terms of digital/binary language is powerful in that it allows engineers to interface basic organic sensors with existing electronics components to produce ultimately usable products. It was believed that this was the first step towards high-throughput production of organic-based digital sensors.

Besides the protocols in terms of logic circuits, the sensing response of OFET gas sensors could also be enhanced by integrating them in oscillator and adaptive amplifier circuits, as reported by Crone, Das *et al.*^{2, 11, 29}

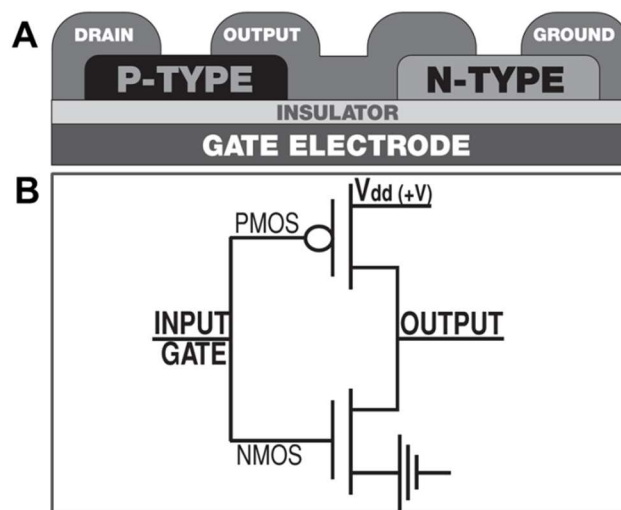


Fig. 16 Intelligent OFET gas sensors capable of digital readouts could be realized using electronic inverter in terms of CMOS-type structure. The device is built up by a combination of a *p*- and an *n*-type OSC of matching μ and V_{Th} . The cross-sectional layout (A) and circuit diagram (B) of the CMOS inverter structure. Copyright 2013, Wiley.

3.5. Interface modification and morphology control

Interface engineering is recognized as a powerful strategy for high-performance OFETs.⁵ From Section 2, we can see that the diagnose principle of OFET transducers could be affected by interfacial modification, especially that occurred at OSC/dielectric interface.^{21, 24, 40} Besides the above-mentioned direct modifications,^{21, 24} a post-treatment of the interface could also be employed to address this issue. A recent example was reported by Zan *et al*, where they demonstrated that pentacene OFETs with their SiO₂ layer modified by PMMA, could display responses in μ , V_{Th} , I_{DS} towards NH₃.⁴⁰ The sensitivity of the device could be further improved distinctly when the PMMA dielectric layer of the corresponding devices was treated by UV irradiation. It was proposed that UV light treatment modified the PMMA functional end-groups from -COOCH₃ to -COOOH, after which the dipole moment of PMMA is increased. This facilitated the absorption of NH₃ and thus brought out boosted sensitivity.

Among various parameters that could affect the performances

of OFETs, the morphology of the OSCs is also considered to be a critical factor,^{1, 6} which could be harnessed for high-quality gas sensors as well. A recent example is proposed by Li *et al.*⁴¹ In this work, ultra-thin dendritic microstripes of 6.5~11 nm based on dialkyl tetrathiapentacene (DTBDT-C6) was assembled in a controllable manner *via* the simple dip-coating method. Noticeably, compared to the OFETs using the continuous films of 20~25 nm of DTBDT-C6 as active layers, thus-fabricated dendritic microstripes-based devices displayed distinctly improved responses with regard to sensitivity, response/recovery time and LOD, towards NH₃. The enhanced sensing performance of the structured OFETs could be attributed to the ultrathin and dendritic morphology features of the microstripes, which provided direct and efficient pathways for full interactions between OSCs and analytes. Considering the fertile achievements in micro/nanostructured molecular assemblies, this protocol, which focuses on micro/nanoarchitected OSCs, provides broad opportunities toward high-quality OFET gas sensors.

4. Gas sensors base on OFET arrays

Among the five major human senses, such as vision, hearing, olfaction, taste and touch, olfaction (sense of smell), by which airborne volatile species are perceived *via* specialized sensory cells of the nasal cavity, is recognized to be the most mysterious and complex one.^{42, 43} Artificial olfaction system, or to say E-nose, which aims at mimicking the perceptive capacity of mammalian olfactory system, is currently a hot topic of broad interest and general concern.^{42, 43} This is owing to its significance in a wide range of multidisciplinary areas, including, but not confined to, disease diagnosis, food/beverage quality control, environmental monitoring, military/security/safety affairs, *etc.* According to the definition given by Gardner and Bartlett, E-nose, also known as artificial nose system, odour/aroma-sensing system, or multi-sensor array *etc.*,^{42, 44, 45} refers to an instrument, which comprises an array of electronic chemical sensors with partial specificity and an appropriate pattern-recognition system, capable of recognizing simple or complex odours.⁴⁵ Actually, the human nose contains approximately 50 million cells in the olfactory epithelium that act as primary receptors to odorous molecules. There are about 10,000 primary neurons associated with these primary receptors that link into a single secondary neuron which in turn feeds the olfactory cortex of the brain.⁴³ As the mammalian olfactory systems are so complex, scientists also called the arrays of gas sensors, which realize their sensing performances in terms of pattern recognition and classification algorithms *via* relevant software, as E-nose, although it is originally proposed to mimic the function of animal nose.^{13, 28, 44} Through the use of a fingerprint response generated by a combinatorial analysis of this sensor array, the specific response of each analyte could consequently be established. Like the mammalian nose, E-nose detects volatile analytes by gas sensor arrays, which transport the sensed information to a recognition organ, for example a computer, which is analogous to human brain. To a great extent, the so-called E-nose in lots of the current literatures is actually a pattern recognition system toward gaseous analytes, which could be simply considered as a multi-sensor array with partial specificity to odorants.

On one hand, the huge achievements of OSCs in terms of

molecular engineering, and the multiple sensing mechanisms endowed by the variety of OSCs, device configuration/dimension, gate dielectric interface modification, and the morphology tunability of the OSC layers, *etc.*, provide OFET gas sensors with tremendous diversity with regard to sensitivity and selectivity. On the other hand, OFET gas sensors are inherently multiparameter electronics, wherein multiple measurement variables could be simultaneously extracted. These issues favor the constructions of gas sensor arrays (the so-called E-nose) based on OFETs, from which rich information concerning the 'fingerprint' of the analytes could be derived. Besides the strategies mentioned in Section 3, the discrimination power of OFET gas sensors could also be improved by combining a number of transistors or a couple of measurement variables in an array, each of which can contribute information for pattern recognition and analyte identification. In this case, the combinatorial responses of the whole array provide a unique fingerprint pattern for analytes.

While independent OFET has witnessed great advancements in gas detection, gas sensors based on OFET arrays have also attracted great attention. A relevant example is reported recently by Bayn *et al.*⁴⁶ In this study, a series of transistors, which used polycyclic aromatic hydrocarbon (PAH) compounds of different coronae and substituents as the OSC layers, were combined to form OFET gas sensor arrays. The results showed that each standalone OFET sensor could display unique responses to a large number of volatile organic compounds (VOCs) of different polarity and aromaticity in terms of a couple of variables such as I_{DS} , μ , V_{Th} and I_{on}/I_{off} . This rendered these interesting sensory arrays capable of generating unique fingerprint for individual analyte. By means of a complementary pattern recognition method, it was found that this sensory system had a powerful ability to: (i) discriminate between aromatic and non-aromatic VOCs; (ii) distinguish polar and non-polar non-aromatic compounds; and to (iii) identify specific VOCs within the subgroups (i.e., aromatic compounds, polar non-aromatic compounds, nonpolar non-aromatic compounds).

Besides derivatives of distinct substituents, different type of OSCs could also be employed to fulfill OFET gas sensor arrays, owing to their distinct responses even toward the same analyte.¹⁵ A typical paradigm is recently presented by Huang *et al*, wherein CuPc (*p*-type OSC), N,N'-dioctyl naphthalenetetracarboxylic diimide (8-NTCDI, *n*-type OSC), and dimethylpropylamine naphthalenetetracarboxylic diimide (DMP-NTCDI) were used to construct OFET sensor arrays.⁴⁷ As expected, CuPc and 8-NTCDI OFETs exhibited opposing responses towards a variety of gaseous analytes. On the other hand, owing to the existence of ionizable side chain, DMP-NTCDI OFETs showed response directions and magnitudes that were not correlated to those of the former two. Specifically, the I_{DS} , μ , and V_{Th} of the devices showed different magnitudes and response directions upon exposure to analytes of different basicity, acidity and polarity (Fig. 17), indicating their strong recognition ability to unambiguously discriminate individual analytes *via* patterned fingerprint. These interesting examples might bring us one step closer to the development of cost-effective, lightweight, low-power, noninvasive OFETs-based tools for the widespread detection of VOCs in real-world applications.^{46, 47}

The above sensory arrays are composed of a set of individual

OFET gas sensors, where diverse variables of the transistors are employed for pattern recognition and analyte identification. These multi-OFETs-multiparameters-based arrays are promising, owing to the accessibility of rich and sophisticated information of the analytes. In these scenarios, tremendous efforts have to be devoted to fabricate various OFETs and analyze the measured data, making the protocol power consumption and time-consuming. Apparently, a single OFET-based sensor array by

taking the advantage of the multiparameter of the transistors, namely, a multiparametric-but-single-OFET-based array, where a set of variables could be extracted concertedly and parallelly, might be an alternative to mitigate these issues to some extent. In this case, besides the frequently used pristine parameters of OFETs, an introduction of new parameters might also add emerging information for pattern recognition.

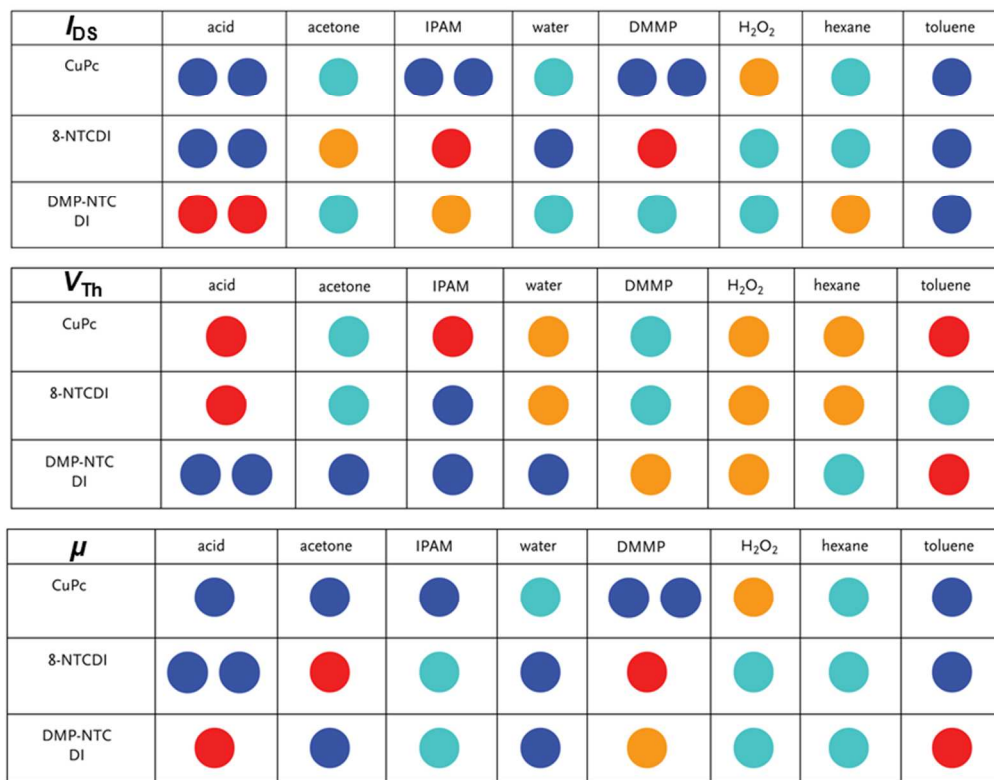


Fig. 17 A representative scenario showing that multi-OFETs-multiparameters-based arrays could work as nice platforms for the discrimination of a large number of VOCs with high selectivity *via* fingerprint pattern recognition. Here, multiparametric responses, such as I_{DS} (top), V_{Th} (middle) and μ (bottom), which are derived from an array of the CuPc, 8-NTCDI, and DMP-NTCDI transistors, are used to establish the map of different analytes. Blue and red spots represent a large decrease and increase, respectively. Two blue and red spots represent a much large decrease and increase, respectively. Orange and light blue spots mean a slight increase and a slight decrease, respectively. Copyright 2013, Wiley.

To address this issue, a dual-modality sensing approach, where two kinds of transduction signals could be generated in concert by an individual sensor, was recently proposed by Wang *et al.*⁴⁸ Here, an light emitting OFET (LEOFET), where poly(2,5-bis(3-alkylthiopen-2-yl)thieno[3,2-b]thiophene) (pBTTT) worked as the first hole transporting layer, tris(8-hydroxyquinoline) aluminum (Alq₃) acted as the electron transport and light emitting layer, and N,N'-di-1-naphthyl-N,N'-diphenyl-1,1'-biphenyl-4,4'-diamine (α -NPD) layer implanted at the pBTTT/Alq₃ interface served as the mediated layer, respectively, was fabricated. The introduction of luminescent OSC layer to the transistor rendered the sensor capable of transducing two different types of gate modulated signals (*viz.*, the intrinsic electrical parameters of OFETs, and the optical/light emission signals) in parallel on the same individual sensor upon exposure to a model analyte 2,3-dimethyl-2,3-dinitrobutane (DMNB). The results showed that the electroluminescent response was more sensitive than the electrical response. This dual dimensional

response might provide a unique dual-variable fingerprint for the target analytes, endowing the sensor with resolving power. In this investigation, only a single model analyte was used to demonstrate the powerful capability of the dual-modal sensing system. However, as a proof-of-concept device, it was believed that upon the full achievement of a multi-mode sensor, it would be possible to assign a unique multi-variable fingerprint to a given target odor in terms of the synergistic coupling of the sensitivities of each mode. Importantly, the access of multiple dimensions of data could render exceptional selectivity to identify target odor out of a mixture.

It can be seen that in contrast to the strategies highlighted in Section 3, OFET gas sensor arrays might be intelligent yet general protocol for gas sensors of high sensitivity and selectivity towards real-world complex gaseous analytes. While promising, it should be noted that no matter which kind of the sensory arrays are, massive amounts of data would be inevitably generated during the operations. Apparently, the collation of this pool of

data is a complex work, wherein diverse algorithms by taking the advantage of the cloud computing and parallel processing are substantially require. This makes it absolutely necessary to collect, analyze and explain these multi-dimensional data to achieve the analyte discrimination *via* pattern recognition, which generally comprises data pre-processing, feature extraction and selection, classifier algorithm-assisted matching, and system accuracy validation *etc.*⁴³

In this regard, the application of suitable pattern recognition algorithms is critical to enhance the sensitivity and selectivity of the sensor arrays. Surya *et al* elaborated on a statistical comparison between different algorithms in classifying empirical multiparametric data that were obtained from the responses of multi-OFETs-multiparameters-based arrays toward a series of explosive vapors.⁴⁹ The results showed that compared to the algorithms such as NaiveBayes (NBS), locally weighted learning (LWL), and sequential minimal optimization (SMO), those based on J48 decision tree displayed the highest accuracy in identifying correctly classified instances. It was believed that such a high accuracy could help develop a basic platform for commercial applications. On the other hand, an appropriate combination of hardware and software is also one of the most important issues that should be taken into account to construct high-performance OFET gas sensors, not matter for an individual OFET or its arrays.^{29, 50} By a coupling of an OFET characterisation circuit based on operational amplifiers (OpAmps) and a data analysis technique using Genetic Programming,⁵⁰ Wedge *et al* reported that sensory arrays based on polytriarylamines OFETs could work as effective vapour sensors with high sensitivity and specificity towards acetone, DMMP, methanol and propan-1-ol. The use of an automated gain method of characterisation, combined with the use of GP-based pattern recognition techniques, permitted a real-time monitoring of gaseous environments with a time-lag of only *ca.* 4 s. It was suggested that the effectiveness of these arrays was originated both from the use of multiple OFETs and from the acquisition of multiple parameters from each OFET.

Whilst making huge progresses, these examples are still far away from those required for mimicking the complex mammalian olfactory system. Nevertheless, accompanied by the intrinsic merits of OFETs mentioned in Section 1, these outstanding results indicate that portable, low-cost, flexible, lightweight, and room temperature workable gas sensors base on OFET arrays might eventually be launched as high-performance E-nose with the development of highly integrated hardware and highly efficient pattern recognition method.

5. Conclusions

Over the last few years, great progresses have been achieved with regard to OFET gas sensors mainly in terms of three aspects, including (i) the sophisticated working principles aiming at providing fundamental knowledge to the sensing processes, (ii) the state-of-the-art strategies targeting at high-performance sensing, and (iii) the advanced gas detection systems in terms of sensory arrays of OFETs intending to construct the so-called E-noses. The rapid development of OFET gas sensors, to a great extent, benefits from the great achievements of the related subjects, such as (a) the *ad-hoc*-designed OSCs, dielectrics,

and/or sensing molecules of specific recognition capacities in terms of molecular design, (b) OFETs in terms of device structure, interfacial modification, crystal engineering, device physical/chemical operation conditions *etc.*, (c) supramolecular chemistry in terms of nanostructured morphology control, and molecular recognition and/or chiral discrimination induced by intermolecular interactions, and (d) hardwares in terms of advanced circuits, and softwares capable of pattern recognition algorithms *etc.* Indeed, the tremendous advancements achieved so far bring the OFET gas sensors a significant step closer to potential applications. Continuous efforts to further improve the overall qualities of this kind of sensors, including sensitivity, specificity and selectivity, response time, stability and reproducibility, limit of detection, capability of digital and intelligent readout, real-time workability, *etc.*, are, however, still strongly desired to meet the requirements of diverse practical uses. In our opinion, the three aspects addressed in the context will continue to be the major subjects of this field.

First, whilst being simple three-terminal organic electronics, the responses of OFET gas sensors could generally be ascribed to complex and multiple mechanisms. Owing to the fertile diversity of the involved materials (OSCs, dielectrics, sensory molecules), device configurations and interfaces, and analytes, *etc.*, it is a difficult work to extract a unified working mechanism. However, it is apparently that an even deeper understanding on the underlying working principles will undoubtedly provide researchers with new and varied opportunities to construct high-quality sensors. Besides, this will also afford important scientific information towards OSCs, such as charge-transport principles, doping and trapping behaviors *etc.*, which are important issues of general concern.

Second, although numerous sophisticated strategies have been proposed to obtain high-performance OFET gas sensors, most of the current works address only one or several aspects of the sensors' quality. It still remains a formidable challenge to construct OFET gas sensors of overall high-qualities, which are substantially needed for practical applications. Obviously, a comprehensive consideration on the individual quality might be necessary when one addresses this subject. On one hand, this needs a deep insight into the working mechanism of the sensors. On the other hand, this could in turn provide nice platforms to disclose the sensing principles, and it might also afford excellent components for the construction of sensory arrays.

Third, whilst being fewer examples in number, compared to the state-of-the-art protocols proposed for individual transistors, OFET sensory arrays favored by the inherent multiparametric feature of the transistors, and also by the abundant availability of diverse OSCs, are verified to be powerful sensing platforms towards real-world complex odours. This approach, however, suffers from the disadvantage that it is a tough work to collect, analyze and explain the generated multi-dimensional data. Meanwhile, with the laboratory fabrication protocols, it is technically difficult to integrate an array of different OFET sensors in the same sensory panel in a large scale manner. Indeed, exciting progresses have been made in this direction by means of a combination of the *ad-hoc*-designed OFET characterization circuit and softwares capable of performing pattern recognition algorithms, there is still a long way to go before fully mimicking

the complex mammalian olfactory system. Joint efforts of hardware and software engineers might be helpful to meet these challenges, favoring the construction of portable yet high-quality odour detection systems of potentially commercial uses.

5 Acknowledgment

This work was supported financially by the National Natural Science Foundation of China (21372225, 20873159), the National Key Basic Research Project of China (2011CB932301).

Notes and references

- ^a Department of Chemistry, School of Science & Collaborative Innovation Center of Chemical Science and Engineering (Tianjin), Tianjin University, Tianjin 300072, People's Republic of China. Fax: +86-22-27403475; Tel: +86-22-27402903; E-mail: chenpl@iccas.ac.cn
- ^b Beijing National Laboratory for Molecular Sciences, Key Laboratory of Organic Solids, Institute of Chemistry, Chinese Academy of Sciences, Beijing 100190, China.
- C. Wang, H. Dong, W. Hu, Y. Liu and D. Zhu, *Chem. Rev.*, 2012, **112**, 2208–2267.
 - Y. Guo, G. Yu and Y. Liu, *Adv. Mater.*, 2010, **22**, 4427–4447.
 - G. Gelinck, P. Heremans, K. Nomoto and T. D. Anthopoulos, *Adv. Mater.*, 2010, **22**, 3778–3798.
 - H. Siringhaus, *Adv. Mater.*, 2014, **26**, 1319–1335.
 - C.-A. Di, Y. Liu, G. Yu and D. Zhu, *Acc. Chem. Res.*, 2009, **42**, 1573–1583.
 - T. Someya, A. Dodabalapur, J. Huang, K. C. See and H. E. Katz, *Adv. Mater.*, 2010, **22**, 3799–3811.
 - A. N. Sokolov, B. C.-K. Tee, C. J. Bettinger, J. B.-H. Tok and Z. Bao, *Acc. Chem. Res.*, 2012, **45**, 361–371.
 - L. Torsi, M. Magliulo, K. Manoli and G. Palazzo, *Chem. Soc. Rev.*, 2013, **42**, 8612–8628.
 - K.-J. Baeg, M. Binda, D. Natali, M. Caironi and Y.-Y. Noh, *Adv. Mater.*, 2013, **25**, 4267–4295.
 - T. Cramer, A. Campana, F. Leonardi, S. Casalini, A. Kyndiah, M. Murgia and F. Biscarini, *J. Mater. Chem. B*, 2013, **1**, 3728–3741.
 - L. Torsi and A. Dodabalapur, *Anal. Chem.*, 2005, **77**, 380A–387A.
 - D. Duarte and A. Dodabalapur, *J. Appl. Phys.*, 2012, **111**, 044509 (7 pp).
 - B. Crone, A. Dodabalapur, A. Gelperin, L. Torsi, H. E. Katz, A. J. Lovinger and Z. Bao, *Appl. Phys. Lett.*, 2001, **78**, 2229–2231.
 - Y. Zang, F. Zhang, D. Huang, C.-A. Di, Q. Meng, X. Gao and D. Zhu, *Adv. Mater.*, 2014, **26**, 2862–2867.
 - R. D. Yang, J. Park, C. N. Colesniuc, I. K. Schuller, J. E. Royer, W. C. Trogler and A. C. Kummel, *J. Chem. Phys.*, 2009, **130**, 164703 (8 pp).
 - J. E. Royer, E. D. Kappe, C. Zhang, D. T. Martin, W. C. Trogler and A. C. Kummel, *J. Phys. Chem. C*, 2012, **116**, 24566–24572.
 - J. H. Park, J. E. Royer, E. Chagarov, T. Kaufman-Osborn, M. Edmonds, T. Kent, S. Lee, W. C. Trogler and A. C. Kummel, *J. Am. Chem. Soc.*, 2013, **135**, 14600–14609.
 - L. Wang, D. Fine, S. I. Khondaker, T. Jung and A. Dodabalapur, *Sens. Actuator B-Chem.*, 2006, **113**, 539–544.
 - L. Wang, D. Fine and A. Dodabalapur, *Appl. Phys. Lett.*, 2004, **85**, 6386–6388.
 - A.-M. Andringa, W. S. C. Roelofs, M. Sommer, M. Thelakkat, M. Kemerink and D. M. de Leeuw, *Appl. Phys. Lett.*, 2012, **101**, 153302 (5 pp).
 - A. Klug, M. Denk, T. Bauer, M. Sandholzer, U. Scherf, C. Slugovc and E. J. W. List, *Org. Electron.*, 2013, **14**, 500–504.
 - T. Shaymurat, Q. Tang, Y. Tong, L. Dong and Y. Liu, *Adv. Mater.*, 2013, **25**, 2269–2273.
 - Y. D. Park, B. Kang, H. S. Lim, K. Cho, M. S. Kang and J. H. Cho, *ACS Appl. Mater. Interfaces*, 2013, **5**, 8591–8596.
 - P. Pacher, A. Lex, V. Proschek, H. Etschmaier, E. Tchernychova, M. Sezen, U. Scherf, W. Grogger, G. Trimmel, C. Slugovc and E. Zojer, *Adv. Mater.*, 2008, **20**, 3143–3148.
 - D. Li, E.-J. Borkent, R. Nortrup, H. Moon, H. Katz and Z. Bao, *Appl. Phys. Lett.*, 2005, **86**, 042105 (3 pp).
 - J. W. Jeong, Y. D. Lee, Y. M. Kim, Y. W. Park, J. H. Choi, T. H. Park, C. D. Soo, S. M. Won, I. K. Han and B. K. Ju, *Sens. Actuator B-Chem.*, 2010, **146**, 40–45.
 - J. Seo, S. Park, S. Nam, H. Kim and Y. Kim, *Sci. Rep.*, 2013, **3**, 2452 (6 pp).
 - L. Torsi, A. Dodabalapur, L. Sabbatini and P.G. Zamboni, *Sens. Actuator B-Chem.*, 2000, **67**, 312–316.
 - A. Das, R. Dost, T.H. Richardson, M. Grell, D. C. Wedge, D. B. Kell, J. J. Morrison and M.L. Turner, *Sens. Actuator B-Chem.*, 2009, **137**, 586–591.
 - A. N. Sokolov, M. E. Roberts, O. B. Johnson, Y. Cao and Z. Bao, *Adv. Mater.*, 2010, **22**, 2349–2353.
 - G. Yang, C.-A. Di, G. Zhang, J. Zhang, J. Xiang, D. Zhang and D. Zhu, *Adv. Funct. Mater.*, 2013, **23**, 1671–1676.
 - Y. Gannot, C. Hertzog-Ronen, N. Tessler and Y. Eichen, *Adv. Funct. Mater.*, 2010, **20**, 105–110.
 - W. Huang, K. Besar, R. LeCover, A. M. Rule, P. N. Breyse and H. E. Katz, *J. Am. Chem. Soc.*, 2012, **134**, 14650–14653.
 - L. Torsi, G. M. Farinola, F. Marinelli, M. C. Tanese, O. H. Omar, L. Valli, F. Babudri, F. Palmisano, P. G. Zamboni and F. Naso, *Nat. Mater.*, 2008, **7**, 412–417.
 - J. Huang, J. Miragliotta, A. Becknell and H. E. Katz, *J. Am. Chem. Soc.*, 2007, **129**, 9366–9376.
 - M. D. Angione, S. Cotrone, M. Magliulo, A. Mallardi, D. Altamura, C. Giannini, N. Cioffi, L. Sabbatini, E. Fratini, P. Baglioni, G. Scamarcio, G. Palazzo and L. Torsi, *Proc. Natl. Acad. Sci. U.S.A.*, 2012, **109**, 6429–6434.
 - B. Li and D. N. Lambeth, *Nano Lett.*, 2008, **8**, 3563–3567.
 - R. D. Yang, J. Park, C. N. Colesniuc, I. K. Schuller, W. C. Trogler and A. C. Kummel, *J. Appl. Phys.*, 2007, **102**, 034515 (7 pp).
 - N. J. Tremblay, B. J. Jung, P. Breyse and H. E. Katz, *Adv. Funct. Mater.*, 2011, **21**, 4314–4319.
 - H.-W. Zan, W.-W. Tsai, Y.-R. Lo, Y.-M. Wu and Y.-S. Yang, *IEEE Sens. J.*, 2012, **12**, 594–601.
 - L. Li, P. Gao, M. Baumgarten, K. Müllen, N. Lu, H. Fuchs and L. Chi, *Adv. Mater.*, 2013, **25**, 3419–3425.
 - S.-W. Chiu and K.-T. Tang, *Sensors*, 2013, **13**, 14214–14247.
 - J. Gutiérrez and M.C. Horriilo, *Talanta*, 2014, **124**, 95–105.
 - M. Ghasemi-Varamkhasti, S. S. Mohtasebi, M. Siadat and S. Balasubramanian, *Sensors*, 2009, **9**, 6058–6083.
 - J. W. Gardner and P. N. Bartlett, *Sens. Actuator B-Chem.*, 1994, **18**, 211–220.
 - A. Bayn, X. Feng, K. Müllen and H. Haick, *ACS Appl. Mater. Interfaces*, 2013, **5**, 3431–3440.
 - W. Huang, J. Sinha, M.-L. Yeh, J. F. M. Hardigree, R. LeCover, K. Besar, A. M. Rule, P. N. Breyse and H. E. Katz, *Adv. Funct. Mater.*, 2013, **23**, 4094–4104.
 - L. Wang and J. S. Swensen, *Sens. Actuator B-Chem.*, 2012, **174**, 366–372.
 - S. G. Surya, R. S. Dudhe, D. Saluru, B. K. Koor, D. K. Sharma and V. R. Rao, *Sens. Actuator B-Chem.*, 2013, **176**, 46–51.
 - D. C. Wedge, A. Das, R. Dost, J. Kettle, M.-B. Madec, J. J. Morrison, M. Grell, D. B. Kell, T. H. Richardson, S. Yeates and M. L. Turner, *Sens. Actuator B-Chem.*, 2009, **143**, 365–372.